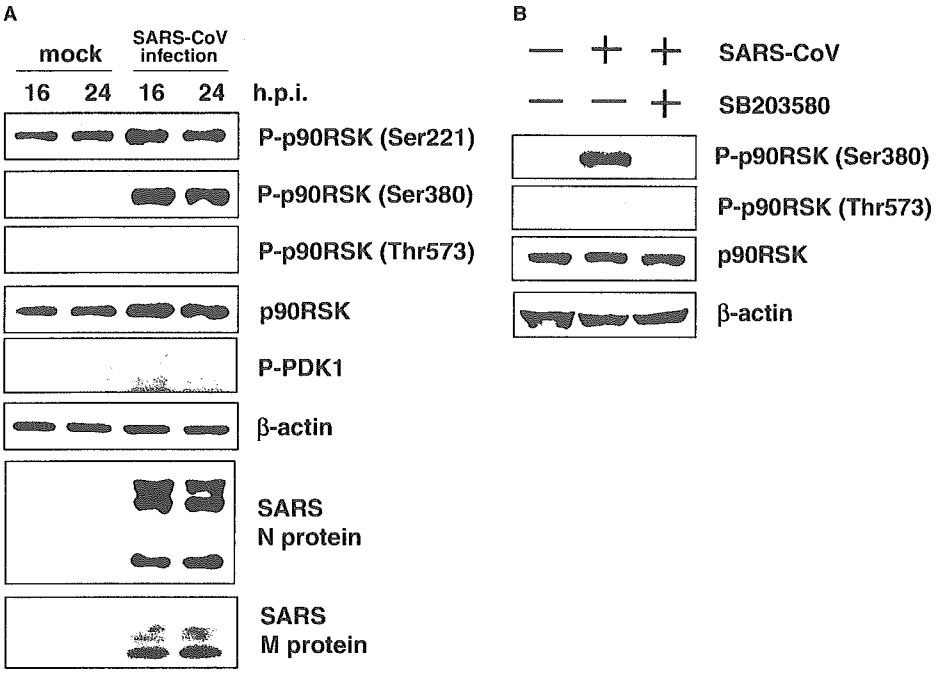

Fig. 5. Phosphorylation of p90RSK in SARS-CoV-infected Vero E6 cells. (A) 1×10^6 cells in 6-well plates were prepared (100% confluency). The cells were infected with SARS-CoV at 50 m.o.i. Western blotting analysis was performed using proteins obtained at 16 and 24 h.p.i. (B) One hour after viral inoculation, cells were treated with SB203580 (20 μM). Proteins were obtained at 24 h.p.i. for Western blotting analysis. Mock-infected cells were treated with DMSO as a control.

important as activation of p90RSK is involved in control of apoptosis.

Thr573 of p90RSK in mock infected cells was phosphorylated by EGF stimulation (Fig. 4A). The Thr573 was slightly phosphorylated in subconfluent mock infected cells compared with confluent mock infected cells (Fig. 4B). However, the phosphorylation was decreased by SARS-CoV-infection and was abolished by the MEK1/2-specific inhibitor, PD98059 (data not shown). Therefore, the ERK signaling pathway is involved in phosphorylation of Thr573 in Vero E6 cells. These observations raise a question regarding the role of ERK in SARS-CoV-infected cells. PD98059-treated SARS-CoV-infected Vero E6 cells showed no significant changes in activated caspase-3 or -7 at 18 h.p.i. (data not shown). This result suggested that phosphorylation of ERK was not sufficient to prevent apoptosis by SARS-CoV infection, as discussed previously regarding the lack of an inhibitory effect on apoptosis due to low activation of Akt in virus-infected cells [27]. Furthermore, we found different phosphorylation kinetics between ERK1 and ERK2 in EGF-treated and SARS-CoV-infected cells. Interestingly, the phosphorylation level of ERK1 is similar to that of ERK2 in SARS-CoV-infected Vero E6 cells (Fig. 1B). Among several experiments, the phosphorylation level of ERK1 was sometimes higher than that of ERK2, as in the case of virus-infected Vero cells at 27 and 44 h.p.i. (Fig. 1B). The total amounts of ERK1 were lower than those of total ERK2 in both mock- and SARS-CoV-infected cells. To confirm that factors contained in seed virus do not upregulate phosphorylation of ERK1, SARS-CoV in seed virus was completely neutralized by anti-SARS-CoV antibody, and then added to cells, resulting in no upregulation of the phosphorylation of ERK1/2 (data not shown). Thus, the strong phosphorylation of ERK1 occurred specifically in SARS-CoV-infected cells. In the case of EGF stimulation, the phosphorylation level of ERK1 was lower than that of ERK2 (Fig. 4A). Eblen et al. showed that ERK2 phosphorylates p90RSK [34]. Angenstein et al. identified p90RSK, ERK2, and GSK-3β as poly-associated proteins, suggesting that polyribosome-bound ERK2 activates p90RSK, and then inhibits GSK-3β [36]. Thus, ERK2 activation is important for phosphorylation of p90RSK in the absence of viral infection. On the other hand, the strong phoshorylation of ERK1 in SARS-CoV-infected cells may affect on phosphorylation status of p90RSK as discussed below.

p90RSK is phosphorylated at Thr573 in the activation loop of the C-terminal kinase domain, and then autophosphorylation at Ser380 in the linker region is thought to be led by this C-terminal kinase domain [11,40]. The phosphorylation level of Ser380 in confluent Vero E6 cells was very low, and SARS-CoV infection induced phosphorylation of Ser380 (Fig. 5). However, as described above, upregulation of Thr573 was not observed in virus-infected cells. There may be differences in regulation of Ser380 in SARS-CoV-infected cells from other stimuli. In the present study, we showed that p38 MAPK can induce phosphorylation of Ser380. Several reports have suggested that p90RSK activation results in phosphorylation of CREB [2,41]. Our previous study showed that SARS-CoV infection of Vero E6 cells induces phosphorylation of CREB, and treatment with SB203580 can inhibit this phosphorylation [24]. Thus, phosphorylation of CREB is regulated by p38 MAPK in SARS-CoV-infected cells. In addition, phosphorylation of ERKs was partially downregulated by treatment with SB203580 in virus-infected cells in viral infected cells (data not shown). Although there is a possibility of

nonspecific reaction by SB203580, cross-talk between ERK and p38 has been reported [37–39]. On the other hand, EGF stimulation induces phosphorylation of ERK without phosphorylation of p38 MAPK (Fig. 4A). Several signaling pathways of p38 MAPK and ERKs including cross-talk may exist in Vero E6 cells. These results may indicate a signaling cascade, p38 MAPK > (ERK >) p90RSK > CREB, in virus-infected cells. Further investigations are necessary to clarify the roles of p90RSK in virus-infected cells.

Based on these results, we conclude that phosphorylation of p90RSK Ser380 is regulated by p38 MAPK, in the absence of upregulation of Thr573 phosphorylation in SARS-CoV-infected cells. These new observations provide valuable insights into the biological effects of p90RSK in SARS-CoV infection.

Acknowledgements: We thank Dr. Funaba (Azabu University, Japan) for helpful suggestions. We also thank Ms. M. Ogata (National Institute of Infectious Diseases, Japan) for her assistance. This work was supported in part by the Japan Health Science Foundation and Grants-in-Aid for Scientific Research, Tokyo, Japan.

References

[1] Pearson, G., Robinson, F., Beers Gibson, T., Xu, B.E., Karandikar, M., Berman, K. and Cobb, M.H. (2001) Mitogen-activated protein (MAP) kinase pathways: regulation and physiological functions. Endocr. Rev. 22, 153–183.

[2] Frodin, M. and Gammeltoft, S. (1999) Role and regulation of 90 kDa ribosomal S6 kinase (RSK) in signal transduction. Mol. Cell. Endocrinol. 151, 65–77.

[3] Moller, D.E., Xia, C.H., Tang, W., Zhu, A.X. and Jakubowski, M. (1994) Human rsk isoforms: cloning and characterization of tissue-specific expression. Am. J. Physiol. 266, C351–C359.

[4] Zhao, Y., Bjorbaek, C., Weremowicz, S., Morton, C.C. and Moller, D.E. (1995) RSK3 encodes a novel pp90rsk isoform with a unique N-terminal sequence: growth factor-stimulated kinase function and nuclear translocation. Mol. Cell. Biol. 15, 4353–4363.

[5] Yntema, H.G., van den Helm, B., Kissing, J., van Duijnhoven, G., Poppelaars, F., Chelly, J., Moraine, C., Fryns, J.P., Hamel, B.C., Heilbronner, H., Pander, H.J., Brunner, H.G., Ropers, H.H., Cremers, F.P. and van Bokhoven, H. (1999) A novel ribosomal S6-kinase (RSK4; RPS6KA6) is commonly deleted in patients with complex X-linked mental retardation. Genomics 62, 332–343.

[6] Bjorbeak, C., Zhao, Y. and Moller, D.E. (1995) Divergent functional roles for p90RSK kinase domains. J. Biol. Chem. 270, 18848–18852.

[7] Fisher, T.L. and Blenis, J. (1996) Evidence for two catalytically active kinase domains in pp90rsk. Mol. Cell. Biol. 16, 1212–1219.

[8] Vik, T.A. and Ryder, J.W. (1997) Identification of serine 380 as the major site of autophosphorylation of xenopus pp90rsk. Biochem. Biophys. Res. Commun. 235, 398–402.

[9] Gavin, A.C. and Nebreda, A.R. (1999) A MAP kinase docking site is required for phosphorylation and activation of $p90^{rsk}$/MAPKAP kinase-1. Curr. Biol. 9, 281–284.

[10] Smith, J.A., Poteet-Smith, C.E., Malarkey, K. and Sturgill, T.W. (1999) Identification of an extracellular signal-regulated kinase (ERK) docking site in ribosomal S6 kinase, a sequence critical for activation by ERK in vivo. J. Biol. Chem. 274, 2893–2898.

[11] Vik, T.A., Sweet, L.J. and Erikson, R.L. (1990) Coinfection of insect cells with recombinant baculovirus expressing pp60v-src results in the activation of a serine-specific protein kinase pp90rsk. Proc. Natl. Acad. Sci. USA 87, 2685–2689.

[12] Frödin, M., Jensen, C.J., Merienne, K. and Gammeltoft, S. (2000) A phosphoserine-regulated docking site in the protein kinase RSK2 that recruits and activates PDK1. EMBO J. 19, 2924–2934.

[13] Jensen, C.J., Buch, M.B., Krag, T.O., Hemmings, B.A., Gammeltoft, S. and Frodin, M. (1999) 90-kDa ribosomal S6 kinase is phosphorylated and activated by 3-phosphoinositide-dependent protein kinase-1. J. Biol. Chem. 274, 27168–27176.

[14] Richards, S.A., Fu, J., Romanelli, A., Shimamura, A. and Blenis, J. (1999) Ribosomal S6 kinase 1 (RSK1) activation requires signals dependent on and independent of the MAP kinase ERK. Curr. Biol. 9, 810–820.

[15] Bonni, A., Brunet, A., West, A.E., Datta, S.R., Takasu, M.A. and Greenberg, M.E. (1999) Cell survival promoted by the Ras-MAPK signaling pathway by transcription-dependent and -independent mechanisms. Science 286, 1358–1362.

[16] Dalby, K.N., Morrice, N., Caudwell, F.B., Avruch, J. and Cohen, P. (1988) Identification of regulatory phosphorylation sites in mitogenactivated protein kinase (MAPK)-activated protein kinase-1a/p90rsk that are inducible by MAPK. J Biol. Chem. 273, 1496–1505.

[17] Buck, M., Poli, V., Hunter, T. and Chojkier, M. (2001) C/EBPβ phosphorylation by RSK creates a functional XEXD caspase inhibitory box critical for cell survival. Mol. Cell 8, 807–816.

[18] Palmer, A., Gavin, A.C. and Nebreda, A.R. (1998) A link between MAP kinase and $p34^{cdc2}$/cyclin B during oocyte maturation: $p90^{rsk}$ phosphorylates and inactivates the $p34^{cdc2}$ inhibitory kinase Myt1. EMBO J. 17, 5037–5047.

[19] Chun, J., Chau, A.S., Maingat, F.G., Edmonds, S.D., Ostergaard, H.L. and Shibuya, E.K. (2005) Phosphorylation of Cdc25C by pp90Rsk contributes to a G2 cell cycle arrest in *Xenopus* cycling egg extracts. Cell Cycle 4, 148–154.

[20] Paronetto, M.P., Giorda, E., Carsetti, R., Rossi, P., Geremia, R. and Sette, C. (2004) Functional interaction between $p90^{Rsk2}$ and Emi1contributes to the metaphase arrest of mouse oocytes. EMBO J. 23, 4649–4659.

[21] Itoh, S., Ding, B., Bains, C.P., Wang, N., Takeishi, Y., Jalili, T., King, G.L., Walsh, R.A., Yan, C. and Abe, J. (2005) Role of p90 ribosomal S6 kinase (p90RSK) in reactive oxygen species and protein kinase Cβ (PKC-β)-mediated cardiac troponin I phosphorylation. J. Biol. Chem. 280, 24135–24142.

[22] Marra, M.A., Jones, S.J., Astell, C.R., Holt, R.A., Brooks-Wilson, A., Butterfield, Y.S., Khattra, J., Asano, J.K., Barber, S.A., Chan, S.Y., Cloutier, A., Coughlin, S.M., Freeman, D., Girn, N., Griffith, O.L., Leach, S.R., Mayo, M., McDonald, H., Montgomery, S.B., Pandoh, P.K., Petrescu, A.S., Robertson, A.G., Schein, J.E., Siddiqui, A., Smailus, D.E., Stott, J.M., Yang, G.S., Plummer, F., Andonov, A., Artsob, H., Bastien, N., Bernard, K., Booth, T.F., Bowness, D., Czub, M., Drebot, M., Fernando, L., Flick, R., Garbutt, M., Gray, M., Grolla, A., Jones, S., Feldmann, H., Meyers, A., Kabani, A., Li, Y., Normand, S., Stroher, U., Tipples, G.A., Tyler, S., Vogrig, R., Ward, D., Watson, B., Brunham, R.C., Krajden, M., Petric, M., Skowronski, D.M., Upton, C. and Roper, R.L. (2003) The genome sequence of the SARS-associated coronavirus. Science 300, 1399–1404.

[23] Rota, P.A., Oberste, M.S., Monroe, S.S., Nix, W.A., Campagnoli, R., Icenogle, J.P., Penaranda, S., Bankamp, B., Maher, K., Chen, M.H., Tong, S., Tamin, A., Lowe, L., Frace, M., DeRisi, J.L., Chen, Q., Wang, D., Erdman, D.D., Peret, T.C., Burns, C., Ksiazek, T.G., Rollin, P.E., Sanchez, A., Liffick, S., Holloway, B., Limor, J., McCaustland, K., Olsen- Rasmussen, M., Fouchier, R., Gunther, S., Osterhaus, A.D., Drosten, C., Pallansch, M.A., Anderson, L.J. and Bellini, W.J. (2003) Characterization of a novel coronavirus associated with severe acute respiratory syndrome. Science 300, 1394–1399.

[24] Mizutani, T., Fukushi, S., Saijo, M., Kurane, I. and Morikawa, S. (2004) Phosphorylation of p38 MAPK and its downstream targets in SARS coronavirus-infected cells. Biochem. Biophys. Res. Commun. 319, 1228–1234.

[25] Mizutani, T., Fukushi, S., Murakami, M., Hirano, T., Saijo, M., Kurane, I. and Morikawa, S. (2004) Tyrosine dephosphorylation of STAT3 in SARS coronavirus-infected Vero E6 cells. FEBS Lett. 577, 187–192.

[26] Mizutani, T., Fukushi, S., Saijo, M., Kurane, I. and Morikawa, S. (2005) JNK and PI3k/Akt signaling pathways are required for establishing persistent SARS-CoV infection in Vero E6 cells. Biochem. Biophys. Acta 1741, 4–10.

[27] Mizutani, T., Fukushi, S., Saijo, M., Kurane, I. and Morikawa, S. (2004) Importance of Akt signaling pathway for apoptosis in SARS-CoV-infected Vero E6 cells. Virology 327, 169–174.

[28] Watanabe, H., de Caestecker, M.P. and Yamada, Y. (2001) Transcriptional cross-talk between Smad, ERK1/2, and p38

mitogen-activated protein kinase pathways regulates transforming growth factor-beta-induced aggrecan gene expression in chondrogenic ATDC5 cells. J. Biol. Chem. 276, 14466–14473.
[29] Surjit, M., Liu, B., Jameel, S., Chow, V.T. and Lal, S.K. (2004) The SARS coronavirus nucleocapsid protein induces actin reorganization and apoptosis in COS-1 cells in the absence of growth factors. Biochem. J. 383, 13–18.
[30] He, R., Leeson, A., Andonov, A., Li, Y., Bastien, N., Cao, J., Osiowy, C., Dobie, F., Cutts, T., Ballantine, M. and Li, X. (2003) Activation of AP-1 signal transduction pathway by SARS coronavirus nucleocapsid protein. Biochem. Biophys. Res. Commun. 311, 870–876.
[31] Tan, Y.J., Fielding, B.C., Goh, P.Y., Shen, S., Tan, T.H., Lim, S.G. and Hong, W. (2004) Overexpression of 7a, a protein specifically encoded by the severe acute respiratory syndrome coronavirus, induces apoptosis via a caspase-dependent pathway. J. Virol. 78, 14043–14047.
[32] Chang, Y.J., Liu, C.Y., Chiang, B.L., Chao, Y.C. and Chen, C.C. (2004) Induction of IL-8 release in lung cells via activator protein-1 by recombinant baculovirus displaying severe acute respiratory syndrome-coronavirus spike proteins: identification of two functional regions. J. Immunol. 173, 7602–7614.
[33] Zeniou, M., Ding, T., Trivier, E. and Hanauer, A. (2002) Expression analysis of RSK gene family members: the RSK2 gene, mutated in Coffin Lowry syndrome, is prominently expressed in brain structures essential for cognitive function and learning. Hum. Mol. Genet. 11, 2929–2940.
[34] Eblen, S.T., Catling, A.D., Assanah, M.C. and Weber, M.J. (2001) Biochemical and biological functions of the N-terminal, noncatalytic domain of extracellular signal-regulated kinase 2. Mol. Cell. Biol. 21, 249–259.
[35] Wang, H.C. and Erikson, R.L. (1992) Activation of protein serine/threonine kinases p42, p63, and p87 in Rous sarcoma virus-transformed cells: signal transduction/transformation-dependent MBP kinases. Mol. Biol. Cell. 3, 1329–1337.
[36] Angenstein, F., Greenough, W.T. and Weiler, I.J. (1998) Metabotropic glutamate receptor-initiated translocation of protein kinase p90rsk to polyribosomes: a possible factor regulating synaptic protein synthesis. Proc. Natl. Acad. Sci. USA 95, 15078–15083.
[37] Xiao, Y.Q., Malcolm, K., Worthen, G.S., Gardai, S., Schiemann, W.P., Fadok, V.A., Bratton, D.L. and Henson, P.M. (2002) Cross-talk between ERK and p38 MAPK mediates selective suppression of pro-inflammatory cytokines by transforming growth factor-β. J. Biol. Chem. 277, 14884–14893.
[38] Mizutani, T., Fukushi, S., Iizuka, D., Inanami, O., Kuwabara, M., Takashima, H., Yanagawa, H., Saijo, M., Kurane, I. and Morikawa, S. Inhibition of cell proliferation by SARS-CoV infection in Vero E6 cells. FEMS Immunol. Med. Microbiol. (in press).
[39] Houliston, R.A., Pearson, J.D. and Wheeler-Jones, C.P.D. (2001) Agonist-specific cross talk between ERKs and $p38^{mapk}$ regulates PGI_2 synthesis in endothelium. Am. J. Physiol. Cell Physiol. 281, C1266–C1276.
[40] Grove, J.R., Price, D.J., Banerjee, P., Balasubramanyam, A., Ahmad, M.F. and Avruch, J. (1993) Regulation of an epitope-tagged recombinant Rsk-1 S6 kinase by phorbol ester and erk/MAP kinase. Biochemistry 32, 7727–7738.
[41] Böhm, M., Moellmann, G., Cheng, E., Alvarez-Franco, M.S.W. and Sassone-Corsi, P.R.H. (1955) Identification of p90RSK as the probable CREB-Ser133 kinase in human melanocytes. Cell Growth Differ. 6, 291 302.

Jpn. J. Infect. Dis., 58, 88-94, 2005

Original Article

Immunological Detection of Severe Acute Respiratory Syndrome Coronavirus by Monoclonal Antibodies

Kazuo Ohnishi, Masahiro Sakaguchi, Tomohiro Kaji, Kiyoko Akagawa, Tadayoshi Taniyama, Masataka Kasai, Yasuko Tsunetsugu-Yokota, Masamichi Oshima, Kiichi Yamamoto, Naomi Takasuka, Shu-ichi Hashimoto, Manabu Ato, Hideki Fujii, Yoshimasa Takahashi, Shigeru Morikawa[1], Koji Ishii[2], Tetsutaro Sata[4], Hirotaka Takagi[5], Shigeyuki Itamura[3], Takato Odagiri[3], Tatsuo Miyamura[2], Ichiro Kurane[1], Masato Tashiro[3], Takeshi Kurata[6], Hiroshi Yoshikura[6] and Toshitada Takemori*

Department of Immunology, [1]Department of Virology I, [2]Department of Virology II, [3]Department of Virology III, [4]Department of Pathology and [5]Division of Biosafety Control and Research, [6]National Institute of Infectious Diseases, Tokyo 162-8640, Japan

(Received October 20, 2004. Accepted February 14, 2005)

SUMMARY: In order to establish immunological detection methods for severe acute respiratory syndrome coronavirus (SARS-CoV), we established monoclonal antibodies directed against structural components of the virus. B cell hybridomas were generated from mice that were hyper-immunized with inactivated SARS-CoV virion. By screening 2,880 generated hybridomas, we established three hybridoma clones that secreted antibodies specific for nucleocapsid protein (N) and 27 clones that secreted antibodies specific for spike protein (S). Among these, four S-protein specific antibodies had in vitro neutralization activity against SARS-CoV infection. These monoclonal antibodies enabled the immunological detection of SARS-CoV by immunofluorescence staining, Western blot or immunohistology. Furthermore, a combination of monoclonal antibodies with different specificities allowed the establishment of a highly sensitive antigen-capture sandwich ELISA system. These monoclonal antibodies would be a useful tool for rapid and specific diagnosis of SARS and also for possible antibody-based treatment of the disease.

INTRODUCTION

The outbreak of severe acute respiratory syndrome (SARS) in 2003, caused by SARS coronavirus (SARS-CoV)(1,2), ultimately led to 8,000 people becoming infected, 916 of whom died (3; http://who.int/csr/sars/country/en/country2003_08_15.pdf). Even though the WHO announced an end to the epidemic (4; http://www.who.int/entity/csr/sars/resources/en/SARSReferenceLab1.pdf), the threat of re-emergence persists due to the absence of a vaccine, and inability of health services to rapidly detect and specifically diagnose the disease. One of the critical issues in the management of clinical patients and control of the pandemic is a system of early diagnosis that distinguishes SARS from other types of pulmonary infections. As an epidemiological history of contact with SARS patients is not always provable and there are no clinical signs unique to SARS patients (5), confirmatory diagnosis relies primarily on laboratory tests.

To date, viral shedding of SARS-CoV has been extensively studied to improve diagnosis and infectious control (6-8). Maximum virus shedding takes place between day 12 and day 14 of disease onset. For most acute respiratory viral infections, viral shedding occurs within the first few days from the nasopharyngeal tissue and soon after at the upper respiratory tract, but seldom lasts for more than 10 days (6-8). The peak of shedding in stools occurs a few days after respiratory shedding and remains high even after 3 weeks (7, 8). SARS-CoV was detected in patients' plasma samples within several days of the onset of fever, sometimes at levels equivalent to those recorded for nasopharyngeal aspirates (6, 9).

Previously, during the outbreak in Hong Kong (8), laboratory diagnosis for SARS virus infection was based on a combination of serologic tests, reverse transcription-polymerase chain reaction (RT-PCR), and virus isolation. IgG seroconversion among those infected was 93% by day 28 (5), suggesting that while antibody seroconversion provides reliable proof of infection (5,10); it is, however, not suitable for early diagnosis (11). Among patients in whom the serological evidence could be retrospectively examined, RT-PCR provided about 60% of the diagnostic yield using tracheal aspirates and stools for the first 2 weeks after the onset of illness (8). Although the availability of data that compares the diagnostic yield of various specimen types is still limited, it has been suggested that a combination of stool samples and pooled throat and nasal swab specimens provides reagents for safe and high-yield SARS-CoV detection (8). Furthermore, in addition to RT-PCR on respiratory and fecal samples, serology is needed to confirm the diagnosis of SARS-CoV infection in most cases.

Based on clinical experience, several options have been considered in the quest to develop the capacity to accurately diagnose SARS-CoV infection, including molecular biology techniques and serological tests such as antigen-captured ELISA assay and immunofluorescence assay to detect virus-infected cells in respiratory swabs (5-12). The preparation of monoclonal antibodies (mAbs) is considered to be valuable especially for serological testing.

*Corresponding author: Mailing address: Department of Immunology, National Institute of Infectious Diseases, Toyama 1-23-1, Shinjuku-ku, Tokyo 162-8640, Japan. Tel: +81-3-5285-1111, Fax: +81-5285-1150, E-mail: ttoshi@nih.go.jp

In this paper we report the successful establishment and the characterization of mAbs against SARS-CoV structural components. These mAbs enabled the general immunological detection of SARS-CoV, by the methods such as immunofluorescent staining, Western blotting, and immunohistology, in addition to the construction of highly sensitive antigen-capture sandwich ELISA.

MATERIALS AND METHODS

Virus and cell culture: SARS-CoV (HKU-39849) was kindly supplied by Dr. J. S. M. Peiris, Department of Microbiology, the University of Hong Kong. The live virus was manipulated under the physical containment level P3. For the purification of the virion, the day-2 culture supernatant of Vero E6, which had been infected with SARS-CoV at moi = 1.0, was centrifuged at 8,000×g for 30 min to remove cell debris. The virion in the supernatant was precipitated with 8% polyethylene glycol/ 0.5 M NaCl, and further purified by 20%/60%-discontinuous sucrose density gradient centrifugation. This fraction was inactivated by UV-irradiation (260 nm, 4.75 J/cm^2), and used as UV-inactivated SARS-CoV fraction. We and others confirmed that this condition completely inactivates SARS-CoV (13,14).

Production of mAbs: BALB/c mice (9-week old females, Japan SLC) were immunized subcutaneously with 20 μg of UV-inactivated SARS-CoV using Freund's Complete Adjuvant (FCA, Sigma, St. Louis, Mo., USA). After 2 weeks, the mice were boosted with a subcutaneous injection of 5 μg of UV-inactivated SARS-CoV using Freund's Incomplete Adjuvant (FIA, Sigma). On day-3 after the boost, sera from the mice were tested by ELISA for the antibody titer against SARS-CoV. The two mice showing highest antibody titer were further boosted intravenously with 5 μg of the inactivated virus 14 days after the previous boost. This immunization schedule was called protocol-1. In protocol-2 the booster injection was repeated two more times before the final boost. Three days after the final boost, spleens from two mice were excised and the splenocytes were fused with Sp2/O-Ag14 myeloma by the polyethylene glycol method of Kozbor and Roder (15). The fused cells from the two spleens were cultured and HAT-selected on twenty 96-well plates. The first screening was conducted by ELISA using SARS-CoV infected Vero E6 cell lysate as the antigen. In this first screening, the ELISA with uninfected Vero E6 cell lysate was used as the negative control. After the virus was inactivated by UV-irradiation, cell lysates were prepared by NP-40 lysis buffer (1% NP-40/ 150 mM NaCl/ 50 mM Tris, pH 7.5) followed by centrifugation at 15,000 rpm for 20 min to remove the cell debris. The supernatant was diluted 100-fold using ELISA-coating buffer (50 mM sodium bicarbonate, pH 9.6) and the ELISA plates (Dynatech, Chantily, Va., USA) were coated at 4°C overnight. After blocking with 1% ovalbumin in PBS-Tween (10 mM phosphate buffer, 140 mM NaCl, 0.05% Tween 20, pH 7.5) for 1 h, the culture supernatants from HAT-selected hybridomas were added and incubated for 1 h. After washing with PBS-Tween, the bound antibodies were detected with alkaline phosphatase-conjugated anti-mouse IgG (1:2000, Zymed, South San Francisco, Calif., USA) using *p*-nitrophenyl phosphate (PNPP) as a substrate. The second screening was conducted by ELISA using the cell lysates of chick embryonic fibroblast (CEF) cell lines that were transfected by vaccinia virus vector containing the gene either of SARS-CoV spike (S) or nucleocapsid (N) proteins.

Recombinant virus proteins: Genomic RNA was extracted from SARS-CoV strain HKU39849 and reverse transcribed to cDNA. The corresponding open reading frames (ORF) to E, M, N and S were amplified by PCR and cloned into the transfer vector, pDIsgptmH5, which also harbored *Escherichia coli* xantine-guanine phosphoribosyltransferase under the control of vaccinia virus p7.5 promoter in the cloning site of pUc/DIs (16). The recombinant clones of attenuated vaccinia virus, DIs, which harbored each ORF were obtained by homologous recombination induced in DIs-infected-, pDIsgptmH5-transfected CEF cells. The detailed protocol will be published elsewhere.

Neutralization assay: The known tissue culture infectious dose (TCID) of SARS-CoV was incubated for 1 h in the presence or absence of the purified mAbs serially diluted 10-fold, and then added to Vero E6 cell culture grown to confluence in a 96-well microtiter plate. As a control, mAbs against N protein was added to the culture. After 48 hr, cells were fixed with 10% formaldehyde and stained with crystal violet to visualize the cytopathic effect induced by the virus (17). Neutralization antibody titers were expressed as the minimum concentration of purified immunoglobulin that inhibits cytopathic effect.

Western blot: UV-inactivated purified SARS-CoV virion (0.5 μg/lane)(13) was loaded on SDS-PAGE under reduced conditions. Proteins were transferred to the PVDF membrane (Genetics, Tokyo, Japan). After blocking with BlockAce (Snow Brand Milk Products Co., Ltd., Tokyo, Japan) reagent, the membranes were reacted with the mAbs or the diluted sera (1:1000) that had been obtained from mice inoculated with UV-irradiated SARS-CoV. After washing, the membrane was reacted with peroxidase-conjugated F(ab')$_2$ fragment anti-mouse IgG (H+L) (1:20,000 Jackson Immuno Research, West Grove, Pa., USA), and the bands were visualized using chemiluminescent reagents (Amasham Biosciences, Piscataway, N.J., USA) on the X-ray film (Kodak, Rochester, N.Y., USA).

Purification and biotinylation of mAbs: Hybridomas were grown in Hybridoma-SFM medium (Invitrogen, Carlsbad, Calif., USA) supplemented with recombinant IL-6 (18) and penicillin (100 U/mL)/streptomycin (100 μg/mL). The culture supernatants were harvested, added with 1/100 volume of 1 M Tris-HCl (pH 7.4) and 1/500 volume of 10% NaN_3, and directly loaded on the Protein G-Sepharose 6B column (Amersham Biosciences). The column was washed with PBS and eluted with Glycine/HCl (pH 2.8). After measuring the OD_{280} of the fractions, protein containing fractions were pooled and added with an equal volume of saturated $(NH_4)_2SO_4$. Precipitated proteins were dissolved in PBS, dialysed against PBS and stored at −20°C. The purified antibodies were biotinylated using sulfo-NHS-LC-biotin (Pierce, Rockford, Ill., USA) according to the manufacturer's protocol.

Antigen-capture ELISA: The purified mAb for the antigen-capture was immobilized on the microplate (Immulon 2, Dynatech) by incubating 4 μg/mL antibody in 50 mM sodium bicarbonate buffer (pH 8.6) at 4°C overnight. The microplate was blocked with 1% BSA, washed with PBS-Tween, and reacted with serial dilution of UV-inactivated purified SARS-CoV for 1 h at room temperature. After washing with PBS-Tween, wells were reacted with biotinylated probing mAb (0.1 μg/mL) for 1 h at room temperature. After washing, wells were reacted with β-D-galactosidase-labeled streptavidine (Zymed) for 1 h at room temperature. After washing,

fluorescent substrate 4-methylumberyferyl-β-D-galactoside (Sigma-Aldrich, St. Louis, Mo., USA) was added and the substrate was incubated for 2 h at 37°C. The reaction was stopped by adding 0.1M Glycine-NaOH (pH 10.2) and the fluorescence (FU) of the reaction product, 4-methylumberiferron, was measured using FluoroScan (Flow Laboratories Inc., Inglewood, Calif., USA).

Histology: Formaldehyde-fixed human lung tissue that was RT-PCR positive for SARS-CoV (19) and lung from a SARS-CoV infected macaque were embedded in paraffin and sectioned using the standard method. After de-paraffinization by standard method, the sections were soaked with 0.1 M citrate-buffer (pH 6.0) and autoclaved for 10 min at 121°C to inactivate viruses. Endogenous peroxidase was inactivated by 0.3% hydrogen peroxide for 30 min at room temperature. After blocking with 5% normal goat serum for 10 min, sections were incubated with the mAb at 4°C overnight. The bound antibody was detected by biotinylated anti-mouse IgG followed by peroxidase-labeled streptavidin (LSAB2 kit, DakoCytomation, Kyoto, Japan) and visualized with 0.2 mg/mL 3,3′-diaminobenzidine in 0.015% hydrogen peroxide/0.05M Tris-HCl (pH 7.6). The sections were counterstained with hematoxylin.

RESULTS

In order to establish the hybridomas that secrete specific mAbs to SARS-CoV, we immunized BALB/c mice with purified SARS-CoV whole virion fraction. The virus was inactivated by UV-irradiation to avoid a change in antigenicity presumably caused by aldehyde-fixation or detergent-solubilization. The immunization protocols used were those of the standard method in which the boost administrations were repeated twice (protocol-1) or four times (protocol-2) with 2-week intervals using FCA/FIA as an adjuvant (see Materials and Methods). Three days after the final boost, a single cell suspension was prepared from two spleens of immunized mice and fused with SP-2/O myeloma by a polyethylene-glycol method, the fused cells were then HAT-selected (15).

In the experiment with immunization protocol-1, we found that the culture supernatants from 28 of the 1,920 wells were strong-positive in ELISA testing in which the cell-lysate of SARS-CoV infected Vero E6 cells was used as a coated antigen (Table 1). As a negative control, we used uninfected Vero E6 cell-lysate as the antigen. Wells that showed a positive reaction were omitted from the count. Among the 28 wells, 19 reacted to vaccinia vector-based recombinant-S-protein and three reacted to recombinant-N-protein. These hybridomas were successfully cloned by a repeated limiting dilution method. The remaining six wells did not give rise to a significant positive signal to recombinant-S, -N or -M proteins. One anti-S mAb cross-reacted to porcine transmissible gastroenteritis virus (TGEV) and this clone was also omitted from further studies. None of these mAbs cross-reacted to mouse hepatitis virus (MHV).

The avidities of these cloned mAbs were tested by avidity-ELISA in the presence of urea. Although in the presence of 6 M urea some anti-S mAbs retained 18-35% of the original reactivity, less than 10% of the original reactivity remained in the presence of 8 M urea (Table 2). Three anti-N mAbs showed a very low avidity index in this assay system.

In a previous report that studied human IgG avidity maturation after rubella vaccination, high-avidity antibodies were defined as those that retain more than 50% of reactivity in the presence of 8 M urea (20). Although it would not be possible to directly apply this definition of polyclonal antibodies to our mAb case, the avidities of mAbs we obtained did not seem particularly high. This prompted us to attempt to obtain better mAbs with higher avidity by repeating booster immunization in anticipation of affinity maturation. After an additional two boosts, hybridomas were established by the same procedure as the first experiment. We screened 960 wells and obtained 14 wells positive for ELISA with SARS-CoV infected Vero E6 cell lysate (Table 1). Among the 14 wells, seven reacted with recombinant-S protein and none of them reacted with recombinant-N or -M proteins. These anti-S antibodies showed significantly higher avidity in the avidity ELISA (two representative clones are shown in Table 2). From the results of this avidity test, we selected five anti-S mAbs that showed the highest avidity index. None of these mAbs cross-reacted to human coronavirus, 229E (data not shown). These five anti-S and three anti-N mAbs were purified, and characterized further.

Table 1. Summary of the first hybridoma screening by ELISA

Immobilized antigen	Experiment-1[1)]	Experiment-2[2)]	Total
(Total wells assayed)	1,920	960	2,880
SARS-CoV infected Vero cell-lysate	28	14	42
Recombinant - S	19	7	26
- N	3	0	3

[1)]: Immunization protocol-1
[2)]: Immunization protocol-2

Table 2. Avidity ELISA

Clone	Epitope	Avidity Index (%)		
		4M urea	6M urea	8M urea
Experiment-1				
SKOT-7	N	1.6	1.2	1.5
SKOT-8	N	2.3	3.2	3.7
SKOT-9	N			
SKOT-3	S	45.5	18.7	1.2
SKOT-10	S	73.4	29.9	2.6
SKOT-20	S	63.8	35.4	8.8
Experiment-2				
SOAT-5	S	51.3	48.0	43.3
SOAT-13	S	77.0	62.0	48.0

All selected mAbs worked successfully in the immunofluorescent staining assay (Fig. 1). Anti-S mAbs such as SKOT-3, -10, -20, SOAT-5 and -13 stained the Golgi body and surface membrane of virus-infected cells but not of uninfected-cells. In contrast, the staining patterns of anti-N mAbs such as SKOT-7, -8 and -9 were mainly confined to the Golgi body.

All anti-N mAbs worked in immunohistochemistry of formalin-fixed, paraffin-embedded sections of both human lung from SARS patients and SARS-CoV infected macaque lung (Fig. 2). The specificity of these stainings was confirmed by the negative results for normal lungs and several specimens from pneumonia patients including cases complicated by measles, influenza type A, herpes-simplex and herpes zoster.

The mAbs that worked for immunohistochemistry, i.e.,

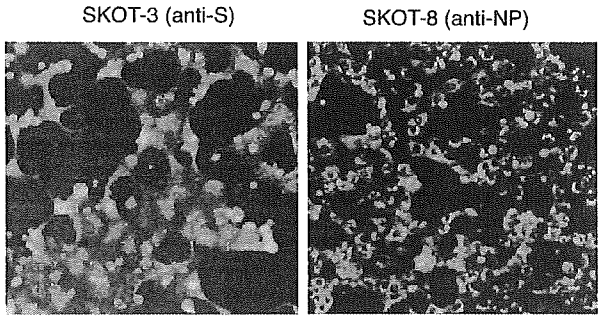

Fig. 1. Fluorescent immunostaining of SARS-CoV infected Vero E6 cells with monoclonal antibodies (mAbs). Parformaldehyde-fixed, SARS-CoV infected Vero E6 cells were permeabilized with TBS-tween and incubated with mAbs from hybridoma clones and the antibodies were detected with FITC-conjugated anti-mouse IgG. Shown are representative staining patterns with anti-S mAb, SKOT-3 (A), and anti-N mAb, SKOT-8 (B).

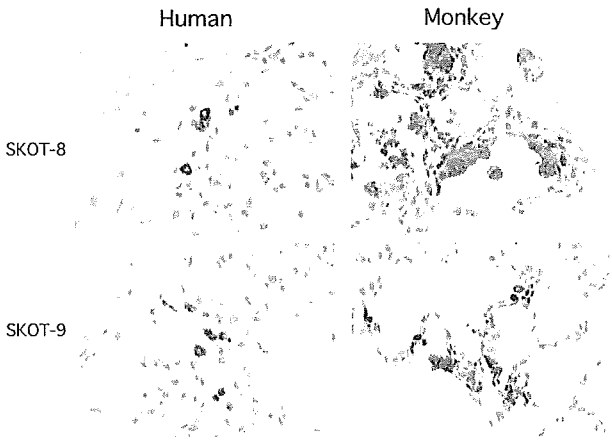

Fig. 2. Immuno-histochemistry of SARS-CoV infected human lung and macaque lung tissues with mAbs. Paraformaldehyde-fixed, paraffin-embedded sections were incubated with mAbs, and then with biotinylated anti-mouse IgG/peroxidase-labeled streptavidin complex before being visualized using DAB as a peroxidase substrate. Counter-staining with hematoxilin. Shown are human patient lung tissue (left panels) and SARS-infected macaque lung tissues (right panels), stained with anti-N mAbs (SKOT-8, SKOT-9).

SKOT-7, -8 and -9 also worked for Western-blot detection of the viral proteins (Fig. 3). Anti-N mAbs detected a band of 50 kDa that corresponds to the calculated molecular weight of SARS-CoV N-protein. In some experiments with longer exposure, a band with an apparent molecular weight of 120 kDa was also detected. None of the anti-S mAbs worked in the Western blot, suggesting that the major antigenic determinants of the S-protein are 'conformational' epitopes.

We tested the in vitro neutralizing activities of anti-S mAbs. As shown in Fig. 4, SKOT-20 neutralized in vitro SARS-CoV infection to Vero E6 cells at an antibody concentration of 1 μg/mL. Another anti-S mAb, SKOT-19, which had a low avidity value, also showed similar neutralizing activity. SKOT-10 and -3 also had neutralization activity but required higher antibody concentrations.

Lastly, we tried to construct an antigen-capture detection system for SARS-CoV by sandwich ELISA. In preliminary experiments, we tested all the combinations of two mAbs from the selected eight mAbs to obtain the highest detection sensitivity for purified SARS-CoV virion, and found that the

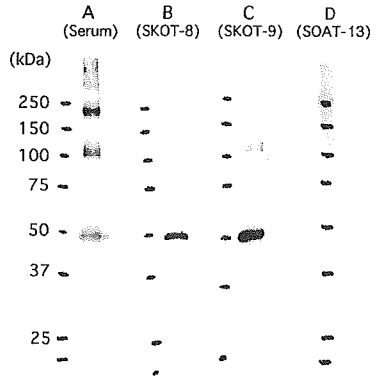

Fig. 3. Detection of virus proteins with Western blot. Purified SARS-CoV proteins (0.5 μg/lane) were electrophoresed with SDS-PAGE under reducing conditions. After blotting on the PVDF membrane, proteins were detected by incubation with mAbs, followed by incubation with peroxidase labeled-F(ab')$_2$ fragment of Donkey anti-mouse IgG. They were then visualized by chemiluminescent reaction. A: mouse serum from SARS-CoV immunized mouse; B: anti-N mAb, SKOT-8; C: anti-N mAb, SKOT-9; D: anti-S mAb, SOAT-13. The positions of molecular weight markers are shown on the left.

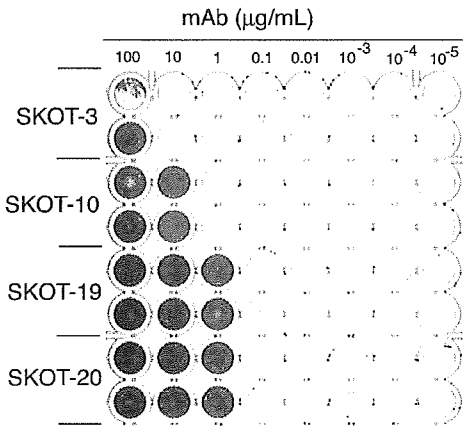

Fig. 4. In vitro neutralization assay of SARS-CoV infection with mAbs. Purified SARS-CoV fraction was diluted to 1×10^3 PFU/mL and incubated with serially-titrated purified mAbs for 1 h at 37°C. After the reaction, samples were poured into wells of a 96-well plate on which Vero E6 cells were grown to 90% confluent. After 48 h, cytotoxicities were visualized by staining the cells with crystalviolet. The results of purified anti-S antibodies (SKOT-3, -10, -19 and -20) with concentrations ranging from 100 μg/mL to 10^{-5} μg/mL are shown.

immobilization of SKOT-8 on the ELISA plate followed by the detection with biotinylated SKOT-9 gave the best result (data not shown; see Materials and Methods). In this sandwich ELISA, SARS-CoV protein was successfully detected in a concentration as low as 40 pg/mL (Fig. 5). Since the mAbs were originally raised against SARS-CoV strain HKU39849, we tested the validity of this system for other strains of SARS-CoV. As shown in Fig. 6, it was confirmed that the strains HK14T1WL, CDC00592 and Frankfurt1 were as detectable as HKU39849 using this system.

DISCUSSION

We established mAbs against SARS-CoV, which enable

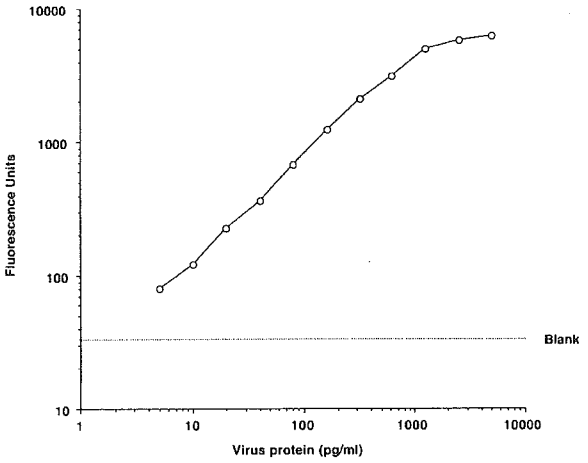

Fig. 5. Antigen-capture ELISA of SARS-CoV with mAbs. Anti-N mAb, SKOT-8, was immobilized on the surface of a 96 well plate. Serially-titrated purified SARS-CoV fractions were reacted for 1 h at room temperature and the bound virus proteins were detected by biotinylated SKOT-9 (anti-N) antibody followed by peroxydase-labeled streptavidin. They were then quantitated by chemiluminescent reaction using 4-methylumberiferril as a substrate. Abscissa: concentration of purified SARS-CoV proteins; ordinate: fluorescent unit.

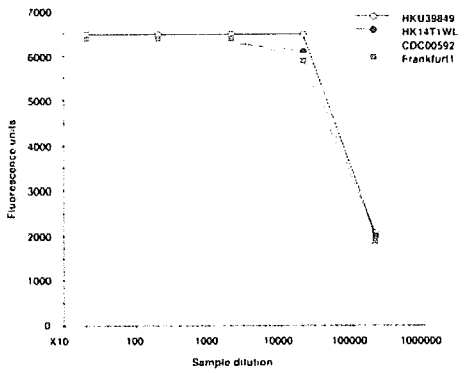

Fig. 6. Comparison of SARS-CoV strains for reactivity to the antigen capture sandwich ELISA. SARS-CoV strains, HKU39849, HK14T1WL, CDC00592 and Frankfurt1 were tested for the reactivity to the antigen-capture ELISA system as described in Fig. 5. Abscissa: sample dilution; ordinate: fluorescent units.

the detection of virus S- and N-proteins by means of immunofluorescence assay, immunohistochemistry, Western blot and antigen-capture ELISA. A summary of selected mAbs is shown in Table 3.

Among the originally selected 42 mAbs that were positive in ELISA for SARS-CoV infected Vero E6 cell lysate, 26 reacted to recombinant-S-protein and only three reacted to N-protein. We could not find hybridoma secreting mAb to M-protein or other protein components of SARS-CoV. These results suggest that S protein is the dominant target in the antibody response. We observed that none of the anti-S mAbs established worked in Western blot, suggesting that these mAbs may recognize 'conformational' epitopes. In contrast, all three anti-N mAbs worked in Western blot and immunohistochemistry, suggesting that these mAbs recognize 'linear' epitopes.

We examined whether our mAbs were applicable for immunofluorescence detection of virus-infected cells. In immunofluorescent staining of Vero E6 cells infected with SARS-CoV, anti-N mAbs stained the Golgi body and anti-S mAbs stained the Golgi body and surface membrane. This difference in localization of N- and S-proteins may reflect the common assembly process of coronaviruses (21). Further analysis is needed to clarify sensitivity and specificity in infected cells for clinical use.

During the course of outbreak of SARS-CoV in Hong Kong, it was reported that more than half the patients were not positively diagnosed by RT-PCR (8). Therefore, the diagnosis was finally confirmed by serum specimens in a convalescent-phase at a late stage of illness (8). To overcome this problem, virus shedding patterns have been extensively analyzed, with results showing that respiratory shedding of the virus increases over the first week and viral shedding in stools begins a few days after respiratory shedding (7,8). From this analysis, it is considered that a combination of stool sampling and pooled throat and nasal swab specimens could be good specimens for safe and highly sensitive SARS-CoV detection.

In general, a single diagnostic test is not conclusively reliable, because of the serious potential for false positives and negatives. Considering the limited sensitivity of RT-PCR, serological screening systems other than antibody detection are currently being examined (22,23). ELISA-based antigen captured assays are known to offer high specificity and reproducibility. Antigen-captured assays have been used in the diagnosis and monitoring of disease in cases of infection with dengue virus (24), human immunodeficient virus p24 (25) and Ebola hemorragic fever (26) and examined in hepatitis B virus and hepatitis C virus (22,23). In this context, extensive analysis in Ebola hemorragic fever suggests that the RT-PCR assay is extremely useful, but should always be utilized in combination with antigen-captured ELISA, which makes the diagnosis more reliable (26).

Table 3. Summary of selected hybridoma clones

Clone	Epitope	Class	IFA	Neutralization[1)]	Western-blot	Histology	Avidity (%)[2)]
SKOT-7	N	IgG	Golgi	-	50kDa	-	1.2
SKOT-8	N	IgG	Golgi	-	50kDa	Usable	3.2
SKOT-9	N	IgG	Golgi	-	120, 50kDa	Usable	3.8
SKOT-3	S	IgG	Golgi / cell membrane	100	-	-	18.7
SKOT-10	S	IgG	Golgi / cell membrane	10	-	-	29.9
SKOT-19	S	IgG	Golgi / cell membrane	1	ND	ND	ND
SKOT-20	S	IgG	Golgi / cell membrane	1	-	-	35.4
SOAT-5	S	IgG	Golgi / cell membrane	ND	-	-	48.0
SOAT-13	S	IgG	Golgi / cell membrane	ND	-	-	62.0

[1)]: Numbers represent minimum concentration (μg/mL) that exerts neutralization. -, no neutralization activity; ND, not determined.
[2)]: Avidity index at 6M urea (see Materials and Methods).

In the case of SARS-CoV, the assay has been recently evaluated by using mAbs and polyclonal antibodies directed against recombinant SARS-CoV nucleocapsid protein (22,23). A soluble N-protein was observed to be released from infected cells in culture, which led to the opportunity to evaluate the level in serum specimens from infected patients. N-antigen ELISA employing mAbs reproducibly detected 50% of patients on days 3 and 5 after the onset of illness, with a limitation of the detection of the recombinant protein at 50 pg/ml (22). N-antigen ELISA with use of polyclonal antibodies detected 60-50% of nasopharyngeal aspirate and fecal specimens from patients at day 3 to day 24 after the onset of illness, although the signal was relatively weak in fecal samples (22). These results suggest that antigen-captured assay could be useful for the early diagnosis of SARS-CoV infection.

We developed an antigen-capture ELISA system that detects purified SARS-CoV virion at levels as low as 40 pg/mL. The sensitivity of the system, which comprised two anti-N mAbs, seems high enough to detect virus protein in patient sera when compared to a recently reported antigen-capture ELISA system, which detects 100 pg/mL of purified recombinant N protein, successfully determined the virus protein in patient sera (22). We are now improving the sensitivity of the system and checking its applicability in the diagnosis and monitoring of SARS-CoV infection. Although none of our mAbs cross-reacted to human or other animal coronaviruses (229E, TGEV and MHV) by ELISA, it is also important to define the specificity of these mAbs by other techniques such as Western blot and immunofluorescent staining. This issue is currently under investigation.

Two anti-S mAbs, SKOT-19 and -20 demonstrated significant virus neutralizing activity. It would be interesting to address whether these mAbs interfere with the binding of the virion to its recently reported receptor, ACE2 (27). If this were the case, the humanization of these mAbs by means of either CDR-grafting or mouse-human chimeric antibody would be of interest as a possible application for the therapeutic use of these mAbs.

ACKNOWLEDGMENTS

We are grateful to Ms. Sayuri Yamaguchi for her assistance in establishing hybridomas.

This work was supported by grant from the Ministry of Health, Labour and Welfare of Japan.

REFERENCES

1. Drosten, C., Gunther, S., Preiser, W., van der Werf, S., Brodt, H. R., Becker, S., Rabenau, H., Panning, M., Kolesnikova, L., Fouchier, R. A., Berger, A., Burguiere, A. M., Cinatl, J., Eickmann, M., Escriou, N., Grywna, K., Kramme, S., Manuguerra, J. C., Muller, S., Rickerts, V., Sturmer, M., Vieth, S., Klenk, H. D., Osterhaus, A. D., Schmitz, H. and Doerr, H. W. (2003): Identification of a novel coronavirus in patients with severe acute respiratory syndrome. N. Engl. J. Med., 348, 1967-1976.
2. Ksiazek, T. G., Erdman, D., Goldsmith, C. S., Zaki, S. R., Peret, T., Emery, S., Tong, S., Urbani, C., Comer, J. A., Lim, W., Rollin, P. E., Dowell, S. F., Ling, A. E., Humphrey, C. D., Shieh, W. J., Guarner, J., Paddock, C. D., Rota, P., Fields, B., DeRisi, J., Yang, J. Y., Cox, N., Hughes, J. M., LeDuc, J. W., Bellini, W. J. and Anderson, L. J. (2003): A novel coronavirus associated with severe acute respiratory syndrome. N. Engl. J. Med., 348, 1953-1966.
3. World Health Organization (2003): Summary table of SARS cases by country, 1 November 2002 - 7 August 2003.
4. World Health Organization: WHO SARS international reference and verification laboratory network: policy and procedures in the inter-epidemic period.
5. Peiris, J. S., Chu, C. M., Cheng, V. C., Chan, K. S., Hung, I. F., Poon, L. L., Law, K. I., Tang, B. S., Hon, T. Y., Chan, C. S., Chan, K. H., Ng, J. S., Zheng, B. J., Ng, W. L., Lai, R. W., Guan, Y. and Yuen, K. Y. (2003): Clinical progression and viral load in a community outbreak of coronavirus-associated SARS pneumonia: a prospective study. Lancet, 361, 1767-1772.
6. Grant, P. R., Garson, J. A., Tedder, R. S., Chan, P. K., Tam, J. S. and Sung, J. J. (2003): Detection of SARS coronavirus in plasma by real-time RT-PCR. N. Engl. J. Med., 349, 2468-2469.
7. Cheng, P. K., Wong, D. A., Tong, L. K., Ip, S. M., Lo, A. C., Lau, C. S., Yeung, E. Y. and Lim, W. W. (2004): Viral shedding patterns of coronavirus in patients with probable severe acute respiratory syndrome. Lancet, 363, 1699-1700.
8. Chan, P. K., To, W. K., Ng, K. C., Lam, R. K., Ng, T. K., Chan, R. C., Wu, A., Yu, W. C., Lee, N., Hui, D. S., Lai, S. T., Hon, E. K., Li, C. K., Sung, J. J. and Tam, J. S. (2004): Laboratory diagnosis of SARS. Emerg. Infect. Dis., 10, 825-831.
9. Poon, L. L., Wong, O. K., Chan, K. H., Luk, W., Yuen, K. Y., Peiris, J. S. and Guan, Y. (2003): Rapid diagnosis of a coronavirus associated with severe acute respiratory syndrome (SARS). Clin. Chem., 49, 953-955.
10. Chen, W., Xu, Z., Mu, J., Yang, L., Gan, H., Mu, F., Fan, B., He, B., Huang, S., You, B., Yang, Y., Tang, X., Qiu, L., Qiu, Y., Wen, J., Fang, J. and Wang, J. (2004): Antibody response and viraemia during the course of severe acute respiratory syndrome (SARS)-associated coronavirus infection. J. Med. Microbiol., 53, 435-438.
11. Nie, Y., Wang, G., Shi, X., Zhang, H., Qiu, Y., He, Z., Wang, W., Lian, G., Yin, X., Du, L., Ren, L., Wang, J., He, X., Li, T., Deng, H. and Ding, M. (2004): Neutralizing antibodies in patients with severe acute respiratory syndrome-associated coronavirus infection. J. Infect. Dis., 190, 1119-1126.
12. Wang, W. K., Chen, S. Y., Liu, I. J., Chen, Y. C., Chen, H. L., Yang, C. F., Chen, P. J., Yeh, S. H., Kao, C. L., Huang, L. M., Hsueh, P. R., Wang, J. T., Sheng, W. H., Fang, C. T., Hung, C. C., Hsieh, S. M., Su, C. P., Chiang, W. C., Yang, J. Y., Lin, J. H., Hsieh, S. C., Hu, H. P., Chiang, Y. P., Yang, P. C. and Chang, S. C. (2004): Detection of SARS-associated coronavirus in throat wash and saliva in early diagnosis. Emerg. Infect. Dis., 10, 1213-1219.
13. Takasuka, N., Fujii, H., Takahashi, Y., Kasai, M., Morikawa, S., Itamura, S., Ishii, K., Sakaguchi, M., Ohnishi, K., Ohshima, M., Hashimoto, S., Odagiri, T., Tashiro, M., Yoshikura, H., Takemori, T. and Tsunetsugu-Yokota, Y. (2004): A subcutaneously injected UV-inactivated SARS coronavirus vaccine elicits systemic humoral immunity in mice. Int. Immunol., 16, 1423-1430.
14. Darnell, M. E., Subbarao, K., Feinstone, S. M. and Taylor, D. R. (2004): Inactivation of the coronavirus that

induces severe acute respiratory syndrome, SARS-CoV. J. Virol. Methods, 121, 85-91.
15. Kozbor, D. and Roder, J. C. (1984): In vitro stimulated lymphocytes as a source of human hybridomas. Eur. J. Immunol., 14, 23-27.
16. Ishii, K., Ueda, Y., Matsuo, K., Matsuura, Y., Kitamura, T., Kato, K., Izumi, Y., Someya, K., Ohsu, T., Honda, M. and Miyamura, T. (2002): Structural analysis of vaccinia virus DIs strain: application as a new replication-deficient viral vector. Virology, 302, 433-444.
17. Storch, G. A. (2001): Diagnostic Virology. p. 493-531. *In* Knipe, D.M., Howley, P.M., (ed.), Fields Virology. 4th ed. Vol. 1. Lippincott Williams & Wilkins, Philadelphia.
18. Karasuyama, H., Rolink, A. and Melchers, F. (1993): A complex of glycoproteins is associated with VpreB/lambda 5 surrogate light chain on the surface of mu heavy chain-negative early precursor B cell lines. J. Exp. Med., 178, 469-478.
19. Nakajima, N., Asahi-Ozaki, Y., Nagata, N., Sato, Y., Dizon, F., Paladin, F. J., Olveda, R. M., Odagiri, T., Tashiro, M. and Sata, T. (2003): SARS coronavirus-infected cells in lung detected by new in situ hybridization technique. Jpn. J. Infect. Dis., 56, 139-141.
20. Hedman, K., Hietala, J., Tiilikainen, A., Hartikainen-Sorri, A. L., Raiha, K., Suni, J., Vaananen, P. and Pietilainen, M. (1989): Maturation of immunoglobulin G avidity after rubella vaccination studied by an enzyme linked immunosorbent assay (avidity-ELISA) and by haemolysis typing. J. Med. Virol., 27, 293-298.
21. Lai, M. M. C. and Holmes, K. V. (2001): *Coronaviridae*: the viruses and their replication. *In* Knipe, D. M. and Howley, P. M. (ed.), Fields Virology. 4th ed. Vol. 1. Lippincott Williams & Wilkins, Philadelphia.
22. Che, X. Y., Qiu, L. W., Pan, Y. X., Wen, K., Hao, W., Zhang, L. Y., Wang, Y. D., Liao, Z. Y., Hua, X., Cheng, V. C. and Yuen, K. Y. (2004): Sensitive and specific monoclonal antibody-based capture enzyme immunoassay for detection of nucleocapsid antigen in sera from patients with severe acute respiratory syndrome. J. Clin. Microbiol., 42, 2629-2635.
23. Lau, S. K., Woo, P. C., Wong, B. H., Tsoi, H. W., Woo, G. K., Poon, R. W., Chan, K. H., Wei, W. I., Peiris, J. S. and Yuen, K. Y. (2004): Detection of severe acute respiratory syndrome (SARS) coronavirus nucleocapsid protein in SARS patients by enzyme-linked immunosorbent assay. J. Clin. Microbiol., 42, 2884-2889.
24. Young, P. R., Hilditch, P. A., Bletchly, C. and Halloran, W. (2000): An antigen capture enzyme-linked immunosorbent assay reveals high levels of the dengue virus protein NS1 in the sera of infected patients. J. Clin. Microbiol., 38, 1053-1057.
25. Sutthent, R., Gaudart, N., Chokpaibulkit, K., Tanliang, N., Kanoksinsombath, C. and Chaisilwatana, P. (2003): p24 Antigen detection assay modified with a booster step for diagnosis and monitoring of human immunodeficiency virus type 1 infection. J. Clin. Microbiol., 41, 1016-1022.
26. Towner, J. S., Rollin, P. E., Bausch, D. G., Sanchez, A., Crary, S. M., Vincent, M., Lee, W. F., Spiropoulou, C. F., Ksiazek, T. G., Lukwiya, M., Kaducu, F., Downing, R. and Nichol, S. T. (2004): Rapid diagnosis of Ebola hemorrhagic fever by reverse transcription-PCR in an outbreak setting and assessment of patient viral load as a predictor of outcome. J. Virol., 78, 4330-4341.
27. Li, W., Moore, M. J., Vasilieva, N., Sui, J., Wong, S. K., Berne, M. A., Somasundaran, M., Sullivan, J. L., Luzuriaga, K., Greenough, T. C., Choe, H. and Farzan, M. (2003): Angiotensin-converting enzyme 2 is a functional receptor for the SARS coronavirus. Nature, 426, 450-454.

CLINICAL AND DIAGNOSTIC LABORATORY IMMUNOLOGY, Apr. 2005, p. 520–524 Vol. 12, No. 4
1071-412X/05/$08.00+0 doi:10.1128/CDLI.12.4.520–524.2005

Persisting Humoral Antiviral Immunity within the Japanese Population after the Discontinuation in 1976 of Routine Smallpox Vaccinations

Shuji Hatakeyama,[1]* Kyoji Moriya,[2] Masayuki Saijo,[3] Yuji Morisawa,[2] Ichiro Kurane,[3] Kazuhiko Koike,[1,2] Satoshi Kimura,[4] and Shigeru Morikawa[3]

Department of Infectious Diseases[1] and Department of Infection Control and Prevention,[2] Graduate School of Medicine, University of Tokyo, Bunkyo-ku, Special Pathogens Laboratory, Department of Virology I, National Institute of Infectious Diseases, Musashimurayama,[3] and AIDS Clinical Center, International Medical Center of Japan, Shinjyuku-ku,[4] Tokyo, Japan

Received 23 November 2004/Returned for modification 13 January 2005/Accepted 17 February 2005

Concerns have arisen recently about the possible use of smallpox for a bioterrorism attack. Routine smallpox vaccination was discontinued in Japan in 1976; however, it is uncertain exactly how long vaccination-induced immunity lasts. We sought to evaluate the seroprevalence and intensity of anti-smallpox immunity among representatives of the present Japanese population. The subjects included 876 individuals who were born between 1937 and 1982. Vaccinia virus-specific immunoglobulin G (IgG) levels were measured by enzyme-linked immunosorbent assay (ELISA), and 152 of 876 samples were also tested for the presence of neutralizing antibodies. Of the subjects who were born before 1962, between 1962 and 1968, and between 1969 and 1975, 98.6, 98.6, and 66.0%, respectively, still retained the vaccinia virus-specific IgG with ELISA values for optical density at 405 nm (OD_{405}) of ≥0.10. The corresponding figures for retained IgGs with OD_{405} values of ≥0.30 were 91.0, 90.3, and 58.2%, respectively. Neutralizing antibodies were also maintained. The sera with OD_{405} values of ≥0.30 showed 89% sensitivity and a 93% positive predictive value for detection of neutralizing antibodies (≥4). Thus, approximately 80% of persons born before 1969 and 50% of those born between 1969 and 1975 were also found to have maintained neutralizing antibodies against smallpox. A considerable proportion of the previous vaccinated individuals still retain significant levels of antiviral immunity. This long-lasting immunity may provide some protective benefits in the case of reemergence of smallpox, and the disease may not spread as widely and fatally as generally expected.

Smallpox was officially declared eradicated by the World Health Organization in 1980 after a worldwide mass vaccination campaign (22). Routine smallpox vaccination was discontinued in Japan in 1976, prior to the declaration. However, concerns have arisen recently about the possible use of variola virus, the causative agent of smallpox, as a bioweapon (14). A total of 37 million Japanese, accounting for approximately 30% of the total population, who were born after the discontinuation of the routine vaccination program are considered to be completely susceptible to smallpox (1), but the immune status of those who were vaccinated decades ago is uncertain. It had been believed that the full protective immunity conferred by smallpox vaccination lasts only 3 to 5 years and that even partial immunity fades substantially after 10 to 20 years (5, 14, 21). Recently, however, it has been suggested that the immunity may last much longer. Several epidemiological studies have shown that immunity to smallpox may still be present many years after the vaccination (8, 13, 15). The degree of residual protection in vaccinated cases was estimated (8) by analyzing data on the outbreak that occurred in Liverpool, in the United Kingdom, during 1902 to 1903 (13) and on smallpox epidemics that occurred following reintroduction to Europe between 1950 and 1971 (15). The authors concluded that protection against fatal smallpox disease was lost at the rate of 0.363% per year and, thus, that 77.6% of vaccinees were still protected even 70 years after vaccination (8). Furthermore, El-Ad et al. reported that the levels of virus-specific neutralizing antibody remain stable for at least 30 years after revaccination (9), and T-cell immunity in response to smallpox vaccination was also reported to remain constant for decades (7, 11).

It has recently been shown that B-cell and T-cell-deficient mice immunized with modified vaccinia virus Ankara, an attenuated vaccinia virus, are both protected against challenge with a pathogenic vaccinia virus, although depletion of a single component of the immune response can reduce the extent of protection (17, 24). In contrast, double-knockout mice deficient in major histocompatibility complex class I and II were not protected (24). These findings indicate that both humoral and cellular immunities make significant contributions to protection against smallpox. With respect to humoral immunities, neutralizing antibodies are believed to play a crucial role in the protection against smallpox (14, 16, 19). Several studies have shown that certain levels of neutralizing antibodies might be involved in preventing the disease or attenuating disease severity (4, 16, 19), although the actual neutralizing antibody titers considered sufficient to protect against smallpox remain to be determined. These data endorse the idea that adequate serum antibody levels might be one of the benchmarks of protective immunity.

* Corresponding author. Mailing address: Department of Infectious Diseases, Graduate School of Medicine, University of Tokyo, 7-3-1 Hongo, Bunkyo-ku, Tokyo 113-8655, Japan. Phone: 81 3 3815 5411 (ext. 33029 or 35335). Fax: 81 3 5800 8806. E-mail: shatake-tky@umin.ac.jp.

If people who were vaccinated some decades ago still maintain some immunity against smallpox, the morbidity, mortality, and transmission rates associated with the disease might be reduced significantly compared with present expectations (3, 18, 20). This might also affect future vaccination policy. Therefore, it is important to clarify whether individuals who were vaccinated decades ago maintain any immunity to smallpox, and if so, what fraction of the population possesses the immunity and how strong the immunity is. We have used enzyme-linked immunosorbent assays (ELISA) and neutralization assays to study the actual prevalence of virus-specific antibodies among representatives of the present Japanese population.

MATERIALS AND METHODS

Study population. We used stored anonymous serum samples that had been obtained from healthcare workers at the University of Tokyo Hospital in 2002 for serological screening of measles, rubella, mumps, and varicella-zoster virus. The sera were stored at 4°C until use. The present study was conducted with the approval of the Institutional Review Board of the University of Tokyo. It was impossible to identify the actual vaccination histories of each individual, because we used anonymous specimens. The ages of the 876 participants (257 males and 619 females) ranged from 20 to 65 years as of 2002 (mean ± standard deviation, 34.4 ± 10.3 years). Routine smallpox vaccination was discontinued in Japan in 1976, and the Immunization Law at that time recommended that individuals should receive three vaccinations against smallpox; the first vaccination was conducted in infancy, and subsequent vaccinations were given at the ages of 6 and 12 years. In this study, therefore, participants were divided into four birth cohorts according to the expected number of smallpox vaccinations they had received: those born after 1975 (younger than 26 years, as of 2002; the never-vaccinated group); those born between 1969 and 1975 (aged 27 to 33 years, as of 2002; the probable once-vaccinated group); those born between 1962 and 1968 (aged 34 to 40 years, as of 2002; the probable twice-vaccinated group); and those born before 1962 (older than 41 years, as of 2002; the probable thrice-vaccinated group). Before 1970, the most widely used strain of smallpox vaccine in Japan was the Ikeda strain, whereas the Lister strain was used during the 1970s.

Detection of vaccinia virus-specific IgG antibodies by ELISA. Levels of specific antibodies against the vaccinia virus, which was used for smallpox vaccines, were measured by ELISA. HeLa cells were infected with the vaccinia virus, Lister strain, at a multiplicity of infection of 1 and cultured for 48 h. They were then lysed in 1 ml of phosphate-buffered saline (PBS) containing 1% NP-40. The lysates were clarified by centrifugation at 10,000 ×*g* for 5 min, and the supernatant fraction was used as a positive vaccinia virus antigen. The mock-infected HeLa cells were also treated in the same way as those being used to prepare the vaccinia virus antigen to produce a negative-control antigen. Half of the wells of a flat-bottomed 96-well ELISA plate (Iwaki, Asahi Techno Glass, Chiba, Japan) were coated with the vaccinia virus-positive antigen, and the other half were coated with the negative-control antigen, followed by incubation at 4°C overnight. Both of the antigens were diluted 1:1,000 with PBS before coating, a dilution level that was determined by preliminary evaluations with box titration using the positive-control serum sample. After being washed three times with PBS containing 0.05% Tween 20 (T-PBS), the wells were blocked with 200 μl of PBS containing 5% skimmed milk and 0.05% Tween 20 (M-T-PBS) for 1 h and then washed three times with T-PBS. Samples of sera (100 μl per well), which were diluted 1:400 with M-T-PBS, were added, and the plates were incubated at 37°C for 1 h. The plates were washed three times with T-PBS and then incubated with 100 μl of M-T-PBS containing horseradish-peroxidase-conjugated goat anti-human IgG antibodies (ZYMED Laboratories, San Francisco, Calif.) (1:1,000 dilution) at 37°C for 1 h. After an additional washing step, 100 μl of the substrate reagent, ABTS [2,2′-azunobis (3-ethylbenzthiazoline sulfonic acid)] solution (Roche Diagnostics, Mannheim, Germany), was added to each well. The plates were incubated at room temperature for 30 min, and the optical density (OD) was measured at a wavelength of 405 nm (OD_{405}) with reference to that at 490 nm. The adjusted OD values (OD_{405}) were calculated by subtracting the OD values of the negative-control-antigen-coated wells from those of the corresponding wells. The negative- and positive-control sera were included for verification in each run.

Vaccinia virus neutralization assay. We conducted the neutralization assay on 152 serum samples, which were randomly selected from each of the birth cohorts (the pre-1962 cohort [n = 49], the 1962-to-1968 cohort [n = 22], the 1969-to-1975 cohort [n = 47], and the post-1975 cohort [n = 34]). Vaccinia virus, Lister strain, and the RK13 cell line grown in Dulbecco's modified Eagle's medium (DMEM) containing 10% fetal calf serum (FCS), penicillin, and streptomycin were used. After heat inactivation at 56°C for 30 min, 100 μl of each of the sera serially diluted fourfold (beginning at 1:4) with DMEM containing 2% FCS and an equal volume of virus suspension containing 100 PFU per 100 μl were mixed and then incubated at 37°C for 2 h. RK13 cell monolayers in 24-well tissue culture plates were inoculated with 100 μl of the mixture in duplicate, and the cells were then incubated at 37°C for 1 h with frequent shaking. Thereafter, the inoculum was removed and the cells were washed once with PBS. They were then cultured in 1 ml of the overlay medium (DMEM containing 2% FCS, penicillin, streptomycin, and 0.5% methylcellulose) at 37°C in a humidified atmosphere of 5% CO_2 in air for 3 days. The cells were fixed with 10% formalin in PBS and stained with 0.1% crystal violet, and the number of plaques was counted. In each assay, the negative- and positive-control sera were included for verification. The neutralizing antibody titer (NT_{50}) was defined as a reciprocal of the highest dilution level of the serum demonstrating a >50% reduction in plaque count compared with the negative control results.

Statistical analysis. The sensitivity, specificity, positive predictive value (PPV), and negative predictive value (NPV) were calculated by standard methods (10). The differences in OD_{405} values and the proportion comparison between the birth cohorts were evaluated by an unpaired Student's t test and chi-square test, respectively, using Stat Flex version 5.0 software (Artech, Osaka, Japan). The level of statistical significance was set at $P < 0.05$. Receiver operating characteristics (ROC) and two-graph ROC (TG-ROC) curves were analyzed using the Stat Flex software. Vaccinia virus-specific NT_{50} values were analyzed by log transformation to linearize the relationship between variables. The relationship between antibody titers determined by neutralization assay and OD_{405} values determined by ELISA was evaluated by linear regression analysis.

RESULTS

Detection of vaccinia virus-specific antibodies by ELISA. We determined the cutoff values in the ELISA for the detection of specific antibodies against vaccinia virus by ROC and TG-ROC curves. The OD_{405} values of sera among subjects who were born in 1977 or after were treated as negative examples, because the routine smallpox vaccination program had already been discontinued. On the other hand, the serum samples of subjects who were born in or before 1968 were treated as positive examples with the vaccination history, because the vaccination program was being strictly enforced at that time, and so the majority of these subjects were considered to have been vaccinated. Logistic regression analysis ROC and TG-ROC curves under the aforementioned conditions are shown in Fig. 1. The cutoff value was set at 0.10, at which level the ELISA system exhibited optimal sensitivity (98.3%) and specificity (99.1%) for detecting the vaccinia virus-specific IgGs elicited by past smallpox vaccination. The area under the ROC curve was 0.988, which corresponds to "excellent probability" (12), allowing us to use this test to distinguish between vaccinated and unvaccinated individuals.

The OD_{405} values that were determined by subjecting serum samples (diluted 1:400) to ELISA are plotted for each birth cohort in Fig. 2A. Of the subjects born before 1962, those born between 1962 and 1968, and those born between 1969 and 1975, 98.6, 98.6, and 66.0%, respectively, retained vaccinia virus-specific IgGs (Table 1). There were significant differences ($P < 0.0001$) in the seropositivity rate between the 1969-to-1975 cohort and the older birth cohorts, but the difference between the 1962-to-1968 cohort and the pre-1962 cohort was not statistically significant ($P = 0.984$). The geometric mean for the OD_{405} values was 1.46 in the pre-1962 cohort, 1.36 in the 1962-to-1968 cohort, and 0.88 in the 1969-to-1975 cohort. Although there was no significant difference in these means

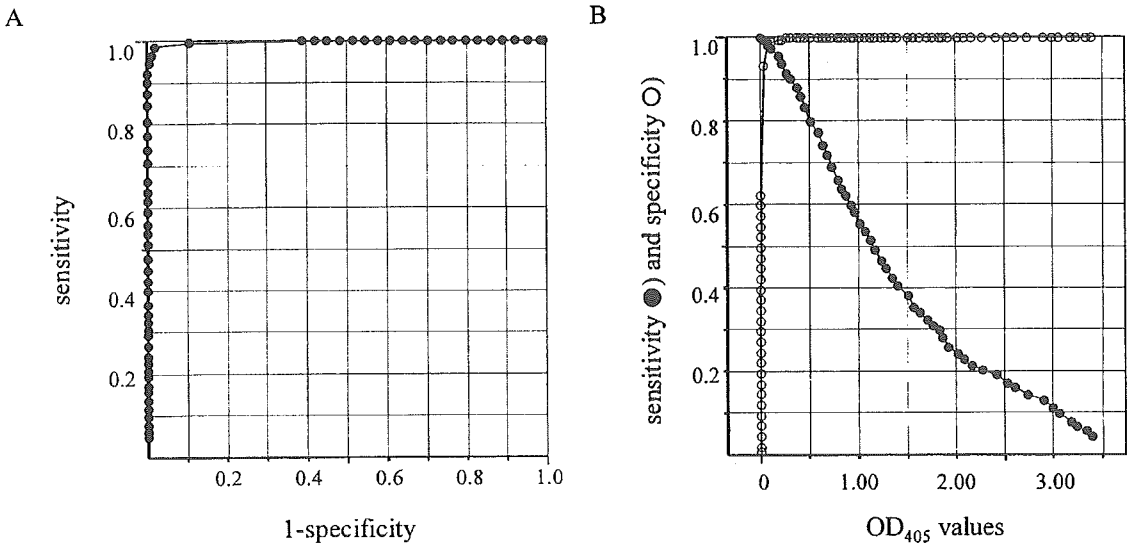

FIG. 1. Receiver operating characteristics (ROC) curve (A) and two-graph-ROC curve (B) for the detection of vaccinia virus-specific IgG. These graphs show the relationship between the sensitivity and specificity of the vaccinia virus-specific ELISA system for each cutoff OD_{405} value. The most optimal sensitivity (98.3%) and specificity (99.1%) are obtained when the cutoff OD_{405} value is set at 0.10. The area under the ROC curve is 0.988, which indicates the test has a good probability of distinguishing between vaccinated and unvaccinated individuals.

between the pre-1962 and 1962-to-1968 cohorts ($P = 0.371$), the mean OD_{405} value for the 1969-to-1975 cohort was significantly ($P < 0.0001$) lower than that for the pre-1969 cohorts (i.e., the pre-1962 and 1962-to-1968 cohorts). The year-on-year seropositivity rate for vaccinia virus-specific IgG among the 1969-to-1975 cohort was 90.0% for 1969 ($n = 29$), 93.3% for 1970 ($n = 30$), 76.2% for 1971 ($n = 42$), 88.6% for 1972 ($n = 44$), 79.3% for 1973 ($n = 58$), 45.8% for 1974 ($n = 48$), and 6.5% for 1975 ($n = 46$). The smallpox vaccination rate in Japan was reported to have already declined sharply in the final few years before the cessation of routine vaccination (information from the Ministry of Health, Labor and Welfare of Japan), which corresponds to the lower seropositivity rate in the 1974 and 1975 birth cohorts of this study. If we took into account the OD_{405} values of the seropositive subjects alone among the 1969-to-1975 cohort (i.e., excluding the seronegative subjects;

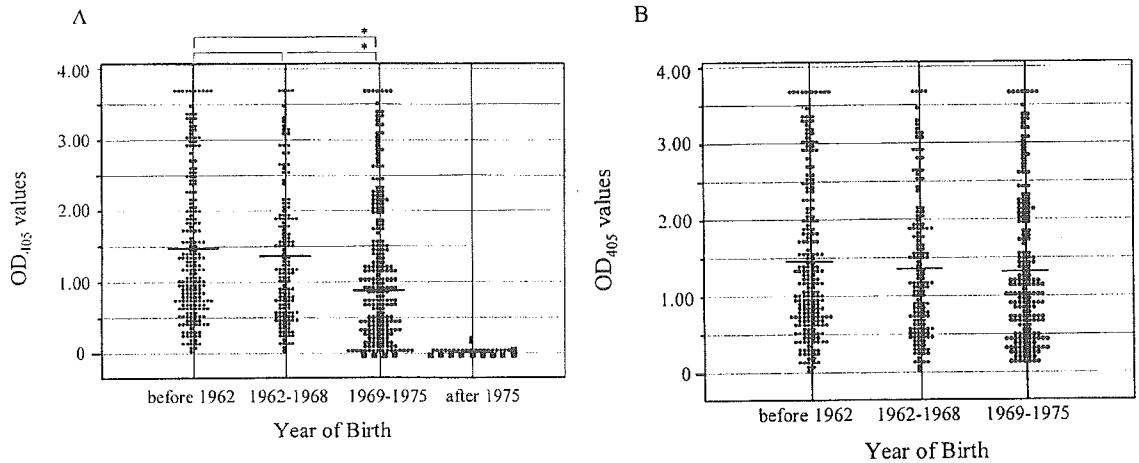

FIG. 2. Vaccinia virus-specific IgG determined by ELISA (the OD_{405} values). Panel A shows the ELISA OD_{405} values in each birth cohort. The bar indicates the geometric mean value, and the actual mean values are 1.46, 1.36, 0.88, and 0.02 for the pre-1962, 1962-to-1968, 1969-to-1975, and post-1975 birth cohorts, respectively. An asterisk indicates that the difference between the mean OD_{405} values is statistically significant. The pre-1962 and 1962-to-1968 cohorts exhibit significantly higher (unpaired Student's t test, $P < 0.0001$) mean OD_{405} values than the other two cohorts, but the difference between those of the pre-1962 and the 1962-to-1968 cohorts is not significant ($P = 0.371$). Each circle corresponds to one subject, and each square represents 20 subjects. Panel B shows the OD_{405} values in the pre-1962, 1962-to-1968, and 1969-to-1975 cohorts. Note, however, that only seropositive samples (OD_{405} values ≥ 0.10) are included for the 1969-to-1975 cohort. The mean values, between which there is no significant difference, are 1.46, 1.36, and 1.39, respectively. IgG, immunoglobulin G; ELISA, enzyme-linked immunosorbent assay; OD_{405}, adjusted optical density.

TABLE 1. Seroprevalence of vaccinia-virus-specific IgG, as determined by ELISA, in four different birth cohorts that cover the period from before 1962 to after the cessation of routine smallpox vaccination in Japan in 1976

Birth yr	No. of subjects	No. (%) of seropositive subjects	
		$OD_{405} \geq 0.10$	$OD_{405} \geq 0.30$
Before 1962	212	209 (98.6)	193 (91.0)
1962–1968	144	142 (98.6)	130 (90.3)
1969–1975	297	196 (66.0)	173 (58.2)
After 1975	223	2 (0.9)	0 (0)
Total	876	548	495

TABLE 2. Sensitivity, specificity, PPV, and NPV of ELISA with the designated reference value for neutralization assay for vaccinia virus within a subsample of 152 sera

ELISA OD_{405}	No. of NT_{50} results		Sensitivity (%)	Specificity (%)	PPV (%)	NPV (%)
	≥4	<4				
≥0.10	96	17	97.0	67.9	85.0	92.3
<0.10	3	36				
≥0.30	88	7	88.9	86.8	92.6	80.7
<0.30	11	46				

OD_{405} values < 0.10), who were unlikely to have been vaccinated, the mean OD_{405} value was 1.32, which was not significantly different from those of the pre-1969 birth cohorts (Fig. 2B).

Relationship between the ELISA and the neutralization assay. Neutralizing antibodies were also maintained, and a significant linear correlation was observed between the neutralizing antibody titers (NT_{50}) and the OD_{405} values determined by the ELISA ($R^2 = 0.450$; $P < 0.0001$) (Fig. 3). The sensitivity, specificity, PPV, and NPV of the ELISA testing for the presence of neutralizing antibodies ($NT_{50} \geq 4$) were 88.9, 86.8, 92.6, and 80.7%, respectively, when the reference OD_{405} value in the ELISA was set at 0.30. The corresponding figures for a reference OD_{405} value of 0.10 were 97.0, 67.9, 85.0, and 92.3%, respectively (Table 2). Neutralizing antibodies were negative ($NT_{50} < 4$) in all of the 34 samples from the post-1975 birth cohort. On the basis of these analyses, the ELISA OD_{405} values of ≥0.10 provide good sensitivity and specificity (98.6 and 99.1%, respectively) for the prediction of smallpox vaccination history, and OD_{405} values of ≥0.30 provide a high PPV (92.6%) for detecting the retention of neutralizing antibodies. The OD_{405} values of ≥0.30 were demonstrated in 91.0% of subjects in the pre-1962 cohort, 90.3% of those in the 1962-to-1968 cohort, and 58.2% of those in the 1969-to-1975 cohort (Table 1). The OD_{405} values were below 0.30 in all samples from the post-1975 birth cohort. These results indicate that approximately 80% of subjects in the pre-1969 birth cohorts, and approximately 50% of those in the 1969-to-1975 cohort, also retained neutralizing antibodies against smallpox.

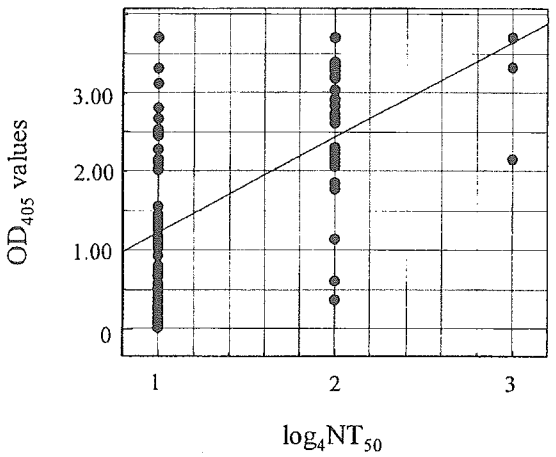

FIG. 3. Relationship between neutralizing antibody titers to vaccinia virus and ELISA OD_{405} values. The regression analysis yields a significant linear relationship ($R^2 = 0.450$; $P < 0.0001$).

DISCUSSION

Neutralizing antibodies have been thought to constitute an important correlate of protective immunity against smallpox (4, 14, 16, 19). To perform a test on a large number of samples, we developed a vaccinia virus-specific ELISA technique with high processing ability, because neutralizing assays are time and labor intensive and are not adequate for handling a large number of samples. Therefore, we evaluated the correlation between antibodies detected by the neutralization assay and those detected by ELISA, because the antibodies detected by ELISA do not always reflect the presence of neutralizing antibodies.

It has been shown that the majority of the Japanese population who were vaccinated against smallpox prior to the cessation of the routine vaccination program in 1976 still maintain certain levels of ELISA-detectable virus-specific antibodies. More than 98% of subjects in the pre-1969 birth cohorts and 66% of those in the 1969-to-1975 cohort still maintained detectable levels of IgG antibodies (OD_{405} values ≥ 0.10). One of the reasons why the subjects in the 1969-to-1975 cohort have a lower seropositivity rate than those in the older cohort is that the vaccination rate per se would have been lower, because they were given only one opportunity to receive a smallpox vaccination. In fact, the smallpox vaccination rate at each stage was reported to be around the 80% level, except in 1974 and 1975, when the rate declined markedly (information from the Ministry of Health, Labor, and Welfare of Japan). The mean OD_{405} value calculated only from the seropositive subjects among the 1969-to-1975 cohort was 1.32, and this value was not significantly different to that of the pre-1962 cohort or the 1962-to-1968 cohort. Although we do not have precise information on how many vaccinations each individual actually received, this result suggests that the additional vaccinations had little influence on the period or degree of IgG retention, as long as the first vaccination had "taken" successfully. Therefore, further investigations are required to determine whether or not multiple smallpox vaccinations are necessary for acquiring significant protection, although it is generally believed that additional vaccinations are likely to confer a stronger and

longer-lasting immune response (2, 9, 23). Hammarlund et al. reported that the mean antibody titer induced by double vaccinations was very slightly but significantly higher than that induced by a single vaccination but that additional (between 3 and 14) vaccinations did not result in any further increase in long-term antibody production (11).

In the present study, most of the individuals whose serum samples exhibited OD_{405} values of ≥ 0.30 also retained the neutralizing antibodies. Thus, it was demonstrated that a considerable proportion of the previously vaccinated individuals still retained neutralizing antibodies. Although lower ELISA OD_{405} values tend to associate with lower neutralizing antibody titers and higher OD_{405} values tend to associate with higher neutralizing antibody titers, the correlation between them was only moderately positive ($R^2 = 0.450$; $P < 0.0001$). It may be due to a number of epitopes on the viral proteins other than neutralizing epitopes on vaccinia virus.

This study has revealed that many individuals who were vaccinated 27 to 53 years ago retain a significant degree of antiviral humoral immunity. Although this remaining immunity may no longer provide full protection, it is highly likely to afford at least partial protection. Hammarlund et al. showed that virus-specific T-cell immunity could persist for a long time after smallpox vaccination, perhaps as long as 75 years, declining only slowly, with a half-life of 8 to 15 years (11). Furthermore, it was shown that virus-specific memory B-cells were maintained for more than 50 years after vaccination and correlated positively with circulating antibody levels (6). In addition, some epidemiological analyses have also indicated that the immunity achieved after smallpox vaccination may remain for several decades (1, 8, 13, 15). Taking these data together, it appears that the immunity conferred by smallpox vaccination persists for longer than had previously been expected.

In the present study, we found that more than 98% of the Japanese population in the pre-1969 birth cohorts and 66% of those in the 1969-to-1975 cohort still maintain the vaccinia virus-specific IgG, whereas approximately 80 and 50%, respectively, also retain detectable levels of neutralizing antibodies. These long-term persisting immunities may provide some protective benefits in the case of intentional smallpox reemergence. In addition, the present results may also contribute in making policy of vaccination priority, especially if vaccine supplies become limited in the event of a widespread outbreak.

ACKNOWLEDGMENTS

We thank M. Ogata, Department of Virology 1, National Institute of Infectious Diseases, Tokyo, Japan, for her technical assistance.

This research was supported in part by a grant-in-aid from the Ministry of Health, Labor, and Welfare of Japan. There is no conflict of interest in connection with this paper.

REFERENCES

1. **Arita, I.** 2002. Duration of immunity after smallpox vaccination: a study on vaccination policy against smallpox bioterrorism in Japan. Jpn. J. Infect. Dis. **55**:112–116.
2. **Bartlett, J., L. Borio, L. Radonovich, J. S. Mair, T. O'Toole, M. Mair, N. Halsey, R. Grow, and T. V. Inglesby.** 2003. Smallpox vaccination in 2003: key information for clinicians. Clin. Infect. Dis. **36**:883–902.
3. **Bozzette, S. A., R. Boer, V. Bhatnagar, J. L. Brower, E. B. Keeler, S. C. Morton, and M. A. Stoto.** 2003. A model for a smallpox-vaccination policy. N. Engl. J. Med. **348**:416–425.
4. **Cherry, J. D., J. D. Connor, K. McIntosh, A. S. Benenson, D. W. Alling, U. T. Rolfe, J. E. Schanberger, and M. J. Mattheis.** 1977. Clinical and serologic study of four smallpox vaccines comparing variations of dose and route of administration. Standard percutaneous revaccination of children who receive primary subcutaneous vaccination. J. Infect. Dis. **135**:176–182.
5. **Cohen, J.** 2001. Bioterrorism. Smallpox vaccinations: how much protection remains? Science **294**:985.
6. **Crotty, S., P. Felgner, H. Davies, J. Glidewell, L. Villarreal, and R. Ahmed.** 2003. Cutting edge: long-term B cell memory in humans after smallpox vaccination. J. Immunol. **171**:4969–4973.
7. **Demkowicz, W. E., Jr., R. A. Littaua, J. Wang, and F. A. Ennis.** 1996. Human cytotoxic T-cell memory: long-lived responses to vaccinia virus. J. Virol. **70**:2627–2631.
8. **Eichner, M.** 2003. Analysis of historical data suggests long-lasting protective effects of smallpox vaccination. Am. J. Epidemiol. **158**:717–723.
9. **el-Ad, B., Y. Roth, A. Winder, Z. Tochner, T. Lublin-Tennenbaum, E. Katz, and T. Schwartz.** 1990. The persistence of neutralizing antibodies after revaccination against smallpox. J. Infect. Dis. **161**:446–448.
10. **Griner, P. F., R. J. Mayewski, A. I. Mushlin, and P. Greenland.** 1981. Selection and interpretation of diagnostic tests and procedures. Principles and applications. Ann. Intern. Med. **94**:557–592.
11. **Hammarlund, E., M. W. Lewis, S. G. Hansen, L. I. Strelow, J. A. Nelson, G. J. Sexton, J. M. Hanifin, and M. K. Slifka.** 2003. Duration of antiviral immunity after smallpox vaccination. Nat. Med. **9**:1131–1137.
12. **Hanley, J. A., and B. J. McNeil.** 1982. The meaning and use of the area under a receiver operating characteristic (ROC) curve. Radiology **143**:29–36.
13. **Hanna, W., and D. Baxby.** 2002. Studies in smallpox and vaccination, 1913. Rev. Med. Virol. **12**:201–209.
14. **Henderson, D. A., T. V. Inglesby, J. G. Bartlett, M. S. Ascher, E. Eitzen, P. B. Jahrling, J. Hauer, M. Layton, J. McDade, M. T. Osterholm, T. O'Toole, G. Parker, T. Perl, P. K. Russell, and K. Tonat.** 1999. Smallpox as a biological weapon: medical and public health management. Working Group on Civilian Biodefense. JAMA **281**:2127–2137.
15. **Mack, T. M.** 1972. Smallpox in Europe, 1950–1971. J. Infect. Dis. **125**:161–169.
16. **Mack, T. M., J. Noble, Jr., and D. B. Thomas.** 1972. A prospective study of serum antibody and protection against smallpox. Am. J. Trop. Med. Hyg. **21**:214–218.
17. **McCurdy, L. H., J. A. Rutigliano, T. R. Johnson, M. Chen, and B. S. Graham.** 2004. Modified vaccinia virus Ankara immunization protects against lethal challenge with recombinant vaccinia virus expressing murine interleukin-4. J. Virol. **78**:12471–12479.
18. **Meltzer, M. I., I. Damon, J. W. LeDuc, and J. D. Millar.** 2001. Modeling potential responses to smallpox as a bioterrorist weapon. Emerg. Infect. Dis. **7**:959–969.
19. **Sarkar, J. K., A. C. Mitra, and M. K. Mukherjee.** 1975. The minimum protective level of antibodies in smallpox. Bull. W. H. O. **52**:307–311.
20. **Smith, G. L., and G. McFadden.** 2002. Smallpox: anything to declare? Nat. Rev. Immunol. **2**:521–527.
21. **World Health Organization.** 1972. W.H.O. Expert Committee on Smallpox Eradication. Second report. WHO Tech. Rep. Ser. **493**:1–64.
22. **World Health Organization.** 1980. Declaration of global eradication of smallpox. Wkly. Epidemiol. Rec. **55**:145–152.
23. **World Health Organization.** 2002. Accession date, 20 November 2004. Smallpox vaccine. [Online.] http://www.who.int/vaccines/en/smallpox.shtml.
24. **Wyatt, L. S., P. L. Earl, L. A. Eller, and B. Moss.** 2004. Highly attenuated smallpox vaccine protects mice with and without immune deficiencies against pathogenic vaccinia virus challenge. Proc. Natl. Acad. Sci. USA **101**:4590–4595.

Published online April 7, 2005

Nucleic Acids Research, 2005, Vol. 33, No. 6 **e65**
doi:10.1093/nar/gni064

Species-independent detection of RNA virus by representational difference analysis using non-ribosomal hexanucleotides for reverse transcription

Daiji Endoh*, Tetsuya Mizutani[1], Rikio Kirisawa[2], Yoshiyuki Maki[3], Hidetoshi Saito[3], Yasuhiro Kon[4], Shigeru Morikawa[1] and Masanobu Hayashi

Laboratory of Veterinary Radiology, School of Veterinary Medicine, Rakuno Gakuen University, Ebetsu 069-8501, Japan, [1]Special Pathogens Laboratory, Department of Virology 1, National Institute of Infectious Diseases, Musashimurayama 208-0011, Japan, [2]Laboratory of Veterinary Microbiology, School of Veterinary Medicine, Rakuno Gakuen University, Ebetsu 069-8501, Japan, [3]Genosys Division, Sigma-Aldrich Japan, Ishikari 061-3241, Japan and [4]Laboratory of Anatomy, Graduate School of Veterinary Medicine, Hokkaido University, Sapporo 060-0818, Japan

Received December 10, 2004; Revised February 26, 2005; Accepted March 18, 2005

ABSTRACT

A method for the isolation of genomic fragments of RNA virus based on cDNA representational difference analysis (cDNA RDA) was developed. cDNA RDA has been applied for the subtraction of poly(A)$^+$ RNAs but not for poly(A)$^-$ RNAs, such as RNA virus genomes, owing to the vast quantity of ribosomal RNAs. We constructed primers for inefficient reverse transcription of ribosomal sequences based on the distribution analysis of hexanucleotide patterns in ribosomal RNA. The analysis revealed that distributions of hexanucleotide patterns in ribosomal RNA and virus genome were different. We constructed 96 hexanucleotides (non-ribosomal hexanucleotides) and used them as mixed primers for reverse transcription of cDNA RDA. A synchronous analysis of hexanucleotide patterns in known viral sequences showed that all the known genomic-size viral sequences include non-ribosomal hexanucleotides. In a model experiment, when non-ribosomal hexanucleotides were used as primers, *in vitro* transcribed plasmid RNA was efficiently reverse transcribed when compared with ribosomal RNA of rat cells. Using non-ribosomal primers, the cDNA fragments of severe acute respiratory syndrome coronavirus and bovine parainfluenza virus 3 were efficiently amplified by subtracting the cDNA amplicons derived from uninfected cells from those that were derived from virus-infected cells. The results suggest that cDNA RDA with non-ribosomal primers can be used for species-independent detection of viruses, including new viruses.

INTRODUCTION

Identifying the causative agent of an infectious disease is the cornerstone for its eventual control. For example, the outbreak of severe acute respiratory syndrome (SARS) was controlled after the identification of the causative agent coronavirus (SARS-CoV) (1). Developments in molecular biological approaches in recent years have led to the identification of many unknown pathogens. Once a fragment from the agent's genome has been isolated and sequenced, standard genomic walking techniques are used to extend the known sequence, and computer homology searches can then be used to identify the likely phylogenetic relationship of the agent with other known organisms (2). Additionally, sequences of some viruses, such as SARS-CoV, have altered during transmission, and this may prevent the detection of the virus by a PCR method (3,4). Thus, a detection method that is not based on the known sequence is essentially required as an alternative method to the normal PCR method.

Representational difference analysis (RDA) is one of the most reliable methods for identifying new agents since it does not require prior knowledge of the agent's class (5). The technique is based on PCR enrichment of DNA fragments that are present in agent-infected cells but absent in normal cells. Using RDA, Chang *et al.* (6) isolated two DNA fragments

*To whom correspondence should be addressed. Tel: +81 11 388 4847; Fax: +81 11 387 5890; Email: dendoh@rakuno.ac.jp

from a Kaposi's sarcoma (KS) lesion in an AIDS patient. The determination of sequences of these fragments resulted in the discovery of the KS-associated herpes virus (7). Despite the fact that RDA has been developed for detecting agents with a DNA-based genome, it can be used to detect the presence or absence of RNA in a sample by generating a cDNA intermediate (cDNA RDA) to amplify the RNA (8). Since a large quantity of ribosomal RNAs interfere with cDNA RDA, the cDNA intermediate should be synthesized from poly(A)$^+$ RNA. Therefore, it is difficult to detect RNA viruses from virus-infected cells by cDNA RDA because many viruses have no poly(A) at the end of the genome. If cDNA RDA can be applied to total RNA without interference with ribosomal RNAs, the virus genome can be amplified from total RNA of virus-infected cells by cDNA RDA.

The selection of poly(A)$^+$ RNA by using an oligo(dT) column followed by oligo(dT) priming can eliminate the influence of ribosomal RNAs on cDNA synthesis. Primers that are specific to a viral genome also efficiently eliminate the influence of ribosomal RNAs. However, prior knowledge of the virus genome is required for the construction of specific primers. In this study, based on the fact that cDNA can be primed with a mixture of oligomers, we constructed a set of oligomers that was inefficient for priming ribosomal RNAs but that normally primed most of the genome of an RNA virus (9,10). Based on the frequency distribution of hexanucleotides in ribosomal RNAs and viral sequences in current public databases, we determined a mixture of 96 hexanucleotides that rarely prime ribosomal RNAs but can prime all the known mammalian viruses listed in public databases. The results of this study show that species-independent detection of viral RNA from infected cells is possible.

MATERIALS AND METHODS

Design and synthesis of a primer mixture

A rat primary transcript, including 18S, 5.8S and 28S ribosomal RNA (V01270.1), was selected for hexanucleotide frequency analysis of ribosomal RNAs. Genomic sequences of SARS-CoV (AY291315) and bovine parainfluenza virus 3 (BPI3, NC_002161) were also selected as representatives of RNA virus (11). We created three programs, GREG, GAS and OSC (produced by C's Labs, Sapporo, Japan and licensed by Sigma–Aldrich Co. Ltd, St Louis, MO), connected to a MySQL database server (version 4.0.20). The program GREG transformed FASTA-formatted sequence to a text-formatted sequence and inserted it into a table in the MySQL database (GREG table). Using these programs, we designed a mixture of hexanucleotide primers. First, sequences were divided into hexamers, and each hexamer was classified into a pattern of hexanucleotide sequence in which $4^6 = 4096$ patterns were included. The program GAS generated frequency distributions of hexanucleotides in the sequences in the GREG table, extracted the progeny with their probabilities of hexanucleotide patterns and inserted them into a table (GAS table) of the database. We made four sets of GREG and GAS tables for rat ribosomal RNAs, a satellite repeat, BPI3 and SARS-CoV (Table 1). The program OSC listed the differences between the two GAS tables, i.e. the program selected oligomer patterns that exist in BPI3 but not in ribosomal RNAs.

Table 1. Probabilities of hexanucleotide patterns in ribosomal RNAs (V01270), a satellite-repeat (V00125), SARS coronavirus (SARS-CoV, AY291315) and bovine parainfluenza virus 3 (BPI3, NC_002161)

Pattern	Probability ($\times 10^{-3}$)			
	Ribosomal RNA	Satellite repeat	BPI3	SARS-CoV
TCTCTC	13.54	1.28	0.25	0.11
AGAGAG	7.53	0.64	0.63	0.16
GAGAGA	7.11	1.92	0.25	0.11
CTCTCT	6.85	0.64	0.33	0.11
TCTGTC	5.67	0.00	0.28	0.25
CTTTCT	4.68	0.32	0.43	0.67
TCTTTC	4.55	0.00	0.46	0.52
TCTCTG	3.55	0.00	0.48	0.21
GTCTCT	3.43	0.64	0.28	0.21
TGTTAA	0.01	0.00	0.43	0.96
GGTCTA	0.01	0.32	0.15	0.16
ATATAT	0.00	0.00	0.96	0.13
GTGCAC	0.00	0.00	0.00	0.27
TAGTAT	0.00	0.00	0.38	0.16
GATATC	0.00	0.00	0.25	0.13
ATACTA	0.00	0.00	0.30	0.28
TATAGT	0.00	0.00	0.35	0.17
TATATA	0.00	0.00	0.81	0.05
ACTATA	0.00	0.00	0.61	0.31

The hexanucleotide patterns are aligned according to the probabilities in ribosomal RNAs. The 10 highest and lowest frequent patterns are listed in the table. A full version of the table, including all patterns, is supplemented online.

The frequency of hexamer patterns in each RNA sequence was transferred into a table of Microsoft Access. A total of 96 hexamer patterns, including those having very low frequencies or those that did not appear in ribosomal RNAs, were synthesized and mixed for use as an RT primer (Table 2, non-ribosomal hexanucleotides).

Database for mammalian viral genomic data

To estimate the frequencies of priming sites with the selected hexanucleotides, we prepared a MySQL table that included sequence data of reported viral genomes as follows. First, we downloaded all viral sequences from the FTP site of EMBL database (release date 30 June 2004) and entered them into tables (EMBL data table) of the MySQL database. The table included EMBL ID, title, annotation and sequence as fields. The annotation field included taxonomic classification of the origin of the data. We separated the words included in the annotation field into taxonomic words, such as family names, and inserted them into a new table (taxonomic table), in which EMBL IDs and taxonomic words were included. We then selected EMBL IDs of mammalian viruses with any of the viral family names listed in Table 5 from the taxonomic table. Next, sequences of mammalian viruses were divided into groups according to their species presented in the taxonomic table. To determine the targets for hexanucleotide analysis, EMBL IDs having the longest sequence in the species were selected as the estimated genomic sequence of the virus, and then, a new table named 'Sequences of viral species' was prepared. Although the longest sequence from each species was selected, some of these sequences were very short. Therefore, we eliminated sequences that were shorter than half of the common genomic size of each viral family. The resultant 1791 viral sequences were inserted into a table titled 'Genomic sequence of viral species'. The frequency of the non-ribosomal hexanucleotides was determined in sense and complementary

Table 2. Hexanucleotide patterns of non-ribosomal hexanucleotides

Motif	Motif	Motif	Motif	Motif	Motif	Motif	Motif
GATATC	GATACT	CGATAT	ACTACT	ATAGTC	CTTAGT	ACTAAG	AACTTA
TAGTAT	CGTATA	GTATAC	TAACGA	CTAGTA	CTTACA	GCATAC	ATAACG
TATAGT	GTATAG	AATCCA	CGACTA	GTACTA	TTATGC	CAATAT	ATGTTA
TATATA	CGGTTA	TAGCAC	TACTAG	TAAGTT	ATACGC	ACCGTA	TGGTAT
ATACTA	AATAGT	ATATCG	AGTAGT	ATATCC	CGCTTA	GTGCTA	TGCGTA
ATATAT	CGCATA	AATATT	GTTAAC	TCGATA	TAACGC	ACGCTA	GGATAT
GTGCAC	ATTACG	TATAGC	GTCTAC	GTACCA	GGTCAT	ATGTCG	CATAGC
ACTATA	TTAACA	CTTGTA	TACAAG	GTATCA	CTCATA	AGCTTA	CATACT
CGTAAT	AGTATC	TAGTCG	TACCAG	ATACTC	AATTTG	CGACAT	CGGATA
CTATAC	TGTTAA	GTAGAC	TGGATT	ACATTA	CTGGTA	GCTATA	TTACTA
TATACG	ACTATT	CTATAG	TCGTTA	ATATTG	TTCATG	GCTATG	ACTCGT
TATGCG	TAACCG	TAGCTA	ATAGTA	CGTCTA	GCGATA	TGTAAG	TAAGGT

strands of the sequences included in the table titled 'Genomic sequence of viral species'.

Culture of virus-infected cells and RNA extraction

The strains SARS-CoV and BPI3 were Frankfurt1 and BN-1, respectively (12–14). SARS-CoV and BPI3 were propagated by serial infection of Vero E6 and MDBK cells, respectively (15).

Vero E6 cells were routinely subcultured in 75 cm^2 flasks in DMEM (Sigma–Aldrich) supplemented with 0.2 mM/ml L-glutamine, 100 U/ml penicillin, 10 μg/ml streptomycin and 5% (v/v) fetal bovine serum (FBS) and maintained at 37°C in an atmosphere of 5% CO_2. For experimental use, the cells were split once in 25 cm^2 flasks and cultured until they reached 100% confluence. Prior to the virus infection, the culture medium was replaced with 2% FBS containing DMEM. SARS-CoV, which was isolated as Frankfurt1 and kindly provided by Dr J. Ziebuhr (16), was used in the present study. The viral infection was established in the cells with a multiplicity of infection (m.o.i) of 10. The infection of cells with SARS-CoV virus and the subsequent treatment of SARS-CoV RNA were restricted in the P4 area in the National Institute of Infectious Disease, and the work with SARS-CoV was performed in accordance with the rules for infectious pathogens that have been notified by the National Institute of Infectious Disease.

MDBK cells were maintained in Eagle's minimum essential medium (Sigma–Aldrich) supplemented with 5% FBS in a humidified atmosphere of 5% CO_2 at 37°C. The cells were infected with BPI3 at an m.o.i of 0.1. The work on infection of BPI3 was performed in accordance with the rules for pathogens that have been notified by Rakuno Gakuen University.

Extraction and *in vitro* synthesis of RNA

Total RNA was isolated using Trizol (Invitrogen, Carlsbad, CA) according to the manufacturer's instructions. Prior to cDNA synthesis, contaminated genomic DNA in the extracted RNA was digested with RNase-free DNase I (Promega, Madison, WI) at 37°C for 1 h. RNA was extracted serially with phenol and chloroform, precipitated with ethanol according to the standard protocol and subsequently used as a control RNA.

For the synthesis of a model RNA, the entire molecule of pCIneo plasmid was transcribed *in vitro* from a T7 promoter. The synthesized 5.4 kb RNA was treated with RNase-free DNase I (Promega), extracted with phenol/chloroform, precipitated with ethanol and subsequently used as a test RNA. After quantitation, the test and control RNAs were mixed to estimate the sensitivity of cDNA RDA in various conditions.

cDNA RDA

First-strand cDNA was synthesized from the mixed RNA with non-ribosomal hexanucleotides by using a double-stranded cDNA synthesis kit (Invitrogen) according to the manufacturer's protocol, i.e. the total RNA was diluted to 1 μg per μl and mixed with dNTPs, the non-ribosomal hexanucleotides, 5× reaction buffer, 0.1 M DTT and an RNase inhibitor. Reverse transcriptase (Superscript II, Invitrogen) was added, and the mixture was incubated at 50°C for 60 min. Second-strand cDNA was synthesized with *Escherichia coli* DNA polymerase (Invitrogen), *E.coli* DNA ligase (Invitrogen) and RNaseH (Invitrogen) at 16°C for 2 h. Double-stranded cDNA was digested with Dpn II, and the resultant fragments were extracted from the digest by using a silicon-membrane-based purification kit (Gene Elute Purification Kit; Sigma–Aldrich).

Linker-derived amplification of DNA fragments and selective amplification steps of cDNA RDA were performed according to the method described by Hubank and Schatz (17). Briefly, 0.1 μg of Dpn II-digested double-stranded cDNA was ligated with RBam24 and RBam12 linkers (5). An aliquot of 1 μl of the ligation solution was diluted with *Taq* mixture (10 μl of 10×*Taq* buffer, including 15 mM $MgCl_2$, and 0.2 mM each of dNTPs). The mixture was preheated to 72°C, and then, *Taq* polymerase (Promega) was added and the mixture was incubated at 72°C for 5 min to synthesize a complementary strand against the overhanging region of RBam24. This was immediately followed by a denaturation step (94°C for 2 min) and 20 cycles of PCR (94°C for 1 min and 72°C for 8 min) to non-specifically amplify 200–800 bp Dpn II-digested cDNA fragments with linkers (amplicons). After amplification, amplicons were redigested with Dpn II and purified with a silicon-membrane-based purification kit to eliminate the spliced linkers. Some amplicons, including the test RNA, were religated with JBam24 and JBam12 linkers. Amplicons with the second linkers were mixed with a large quantity of amplicons without the test RNA sequences.

The mixture was precipitated with ethanol and 3 M sodium acetate, dissolved in 4 µl of 3× EE buffer {30 mM EPPS [*N*-(2-hydroxyethyl)piperazine-*N'*-3-propanesulfonic acid], 3 mM EDTA, pH 8.0} and covered with mineral oil. After the mixture was heated to 99°C for 4 min, 1 µl of 5 M NaCl was added, and the solution was incubated at 67°C for 21 h. During this incubation period, amplicons from normal cellular RNA with a linker included in the test amplicons were hybridized with those from uninfected cells without a linker. After hybridization, the reaction mixture was diluted to 100 µl with reaction buffer of *Taq* DNA polymerase (Promega) as described above. Amplicons having the linker sequence at both ends were amplified by a denaturation step (94°C for 2 min) and 20 cycles of PCR (94°C for 1 min and 72°C for 3 min).

RNAs extracted from virus-infected cells were subjected to cDNA RDA as described above, by using amplicons synthesized from RNA obtained from uninfected cells.

Southern blot hybridization

cDNA RDA-derived fragments in quantities ranging from 100 ng to 2 µg were separated on agarose gels, blotted onto a Biodyne nylon membrane (Pall Co. Ltd, Port Washington, NY) by capillary transfer in 20× SSC (3 M sodium chloride and 0.3 M sodium citrate) for 16 h and fixed to the membrane by baking in an oven at 80°C for 30 min. pCIneo was used as a probe for the *in vitro* synthesized RNA. A random primer labelling kit (BcaBest Labeling kit, Takara Shuzo Co. Ltd, Kyoto, Japan) was used for labelling with ^{32}P and hybridized in SuperHybPlus hybridization solution (Sigma–Aldrich) according to the manufacturers' protocol.

Although amplicons are cloned into a vector to identify its sequence, according to 'Cartagena Protocol on Biosafety Text of the Protocol', amplicons from SARS-CoV-infected cells should not be cloned into any plasmid. Therefore, by performing hybridization, we identified that the sequences of amplicons derived from SARS-CoV-infected cells were identical to SARS-CoV. To determine probes for SARS-CoV, the PCR products predicted from the genomic sequence and sizes of cDNA RDA products were amplified from the SARS-CoV genome. These PCR products were purified, labelled with DIG and independently hybridized using a slit of the nylon membrane blotted with amplicons derived from SARS-CoV-infected cells. DIG labelling and hybridization were carried out according to the manufacturer's instructions provided with the DIG-hybridization kit (F. Hoffmann-La Roche Ltd, Diagnostics Division, Basel, Switzerland). Hybridization was carried out with DIG-labelled DNA probes at 65°C for 16 h in DIG-hybridization solution.

Cloning and sequence analysis

The cDNA RDA-derived fragments were respliced with Dpn II, separated on agarose gels, extracted with a silicon-membrane-based purification kit and cloned into pSPORT1 (Invitrogen). Plasmids that included cDNA RDA-derived fragments were selected by colony PCR and purified with a silicon-membrane-based purification kit. Three clones of the plasmid were sequenced along with the fragment to detect PCR errors. Sequences of the cDNA RDA-derived fragments were determined using a DYEnamic ET-terminator kit (Amersham Biosciences Corp., Piscataway, NJ) and an ABI Prism 310 sequencer (PerkinElmer Life and Analytical Sciences, Inc., Boston, MA) with M13 forward and reverse primers (Takara Shuzo). We used the BLAST program on NCBI to determine sequences that were homologous to the isolated fragments.

RESULTS

Frequency distribution of hexanucleotides within the ribosomal sequences

To predict the major RNA molecule in cellular RNA, we synthesized cDNA from RNA extracted from normal bovine cells, synthesized amplicons by using random primers, spliced them with Dpn II and finally subcloned them into pSPORT1. Among the sequences of 30 selected clones, the sequences of 25 clones and 5 clones were highly homologous to those of ribosomal RNA and a 1399 bp satellite repeat (GenBank accession no. V00125), respectively. Based on this result, ribosomal and satellite sequences were determined for analysing hexanucleotide frequency. Since the reported ribosomal sequences of mammals are highly homologous to each other, we selected rat premature 18S, 5.8S and 28S ribosomal sequences as ribosomal sequences for hexanucleotide frequency analysis. Genome sequences of SARS-CoV and BPI3 were selected as representatives of RNA viral sequence. Table 1 shows the probabilities [number of the patterns/(length of sequence × 2)] of hexanucleotides in the human ribosomal RNA, V00125 satellite repeat, BPI3 and SARS-CoV. If a random sequence is assumed, frequencies would be distributed according to the Poisson's distribution, and the average of frequency would be the same as the variance of frequency. Although the average/variance ratios of all the four sequences were <1, the ratio of ribosomal RNA was smallest in these sequences (Table 3). This value suggests that the probabilities of hexamer patterns of ribosomal RNA were strongly biased from random sequence. Based on histograms of probabilities, the distribution of the probabilities of hexamer patterns in ribosomal RNA differed greatly from those of V00125 satellite repeat or BPI3 (Figure 1). It should be noted that 8 hexanucleotides did not exist and over 90 hexanucleotides were rare in the ribosomal sequence. To determine primer sequences that do not prime ribosomal RNA but prime viral RNA, the probabilities of hexamer patterns in ribosomal RNA and satellite repeat were calculated. The hexamer patterns were then realigned in an ascending order according to the sum of probabilities, and the 1st to 96th patterns were selected as non-ribosomal hexanucleotides, i.e. we selected 96 rarest hexanucleotide patterns (Table 2, non-ribosomal hexanucleotides) in major transcripts in normal mammalian cells on the assumption that ribosomal RNA and transcripts from satellites are the most frequent transcripts in normal cells.

Table 3. Average and variances of frequencies of hexanucleotide patterns in ribosomal RNAs, a satellite repeat (V00125), bovine parainfluenza virus 3 (BPI3) and SARS coronavirus (SARS-CoV)

	Ribosomal RNAs	Satellite repeat	BPI3	SARS-CoV
Average	26.8	1.9	10.6	18.6
Variance	2156.5	2.5	96.0	188.1
Average/variance	0.012	0.76	0.11	0.099

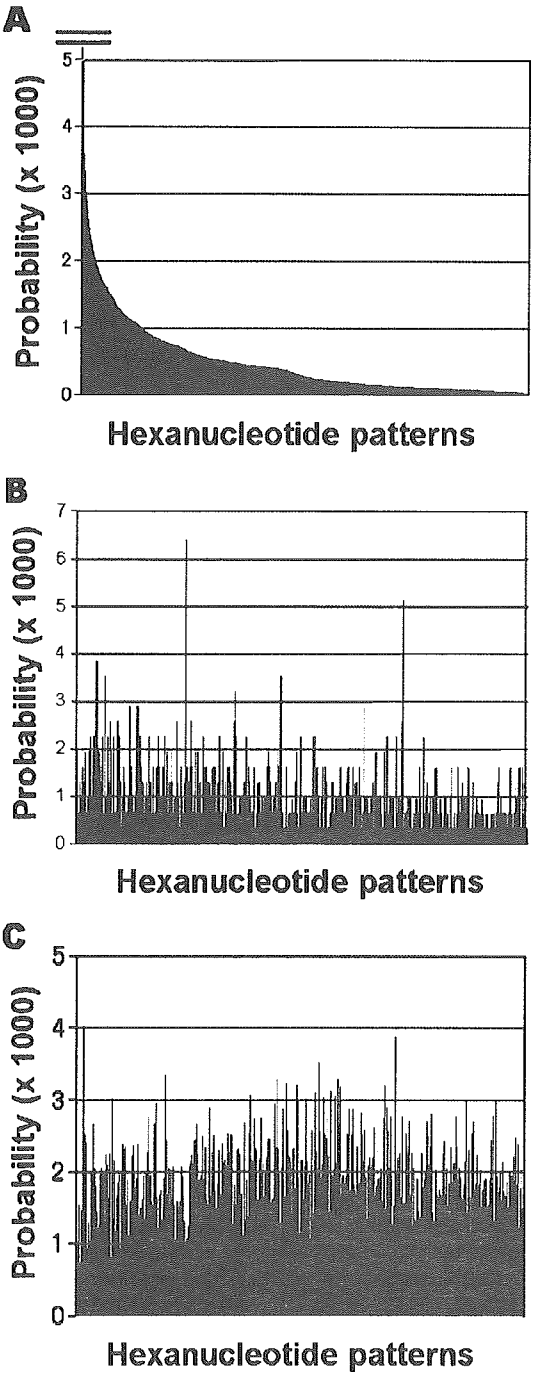

Figure 1. Histogram of probabilities of hexanucleotide patterns in ribosomal RNAs (**A**), a satellite repeat (**B**), BPI3 and SARS-CoV (**C**). From each sequence, the frequency was determined for each hexanucleotide pattern by using programs described in Materials and Methods. Probability was calculated as (frequency of a motif/total length of sequence). For simple comparison, the probabilities of ribosome RNAs and satellite repeat or SARS-CoV and BPI3 were added for each hexanucleotide pattern. Hexanucleotide patterns were aligned according to their probability in the ribosomal RNAs. When the probabilities of hexanucleotide patterns were larger than 0.005, the data were omitted.

The rarity of non-ribosomal hexanucleotides in comparison with non-V00125-satellite and random hexamers was confirmed in reported sequences of mammalian ribosomal RNAs (Table 4). The probabilities were relatively low in all the mammalian ribosomal sequences reported in GenBank. It is considered that non-ribosomal hexanucleotides inefficiently primed ribosomal RNAs in reverse transcription. On the other hand, the probabilities of non-ribosomal, non-V00125-satellite or random hexamers were different among the satellite sequences.

Frequencies of non-ribosomal hexanucleotides in viral genomic sequences

In addition to the inefficiency to prime ribosomal RNAs, efficient priming of V00125-satellite-repeat and BPI3 with non-ribosomal hexanucleotides is shown in Figure 1. To predict priming efficiency in many viruses, the probability of non-ribosomal hexanucleotides in known viral genomes was estimated. In 1791 viral sequences in 'Genomic sequences of viral species', the median probabilities of non-ribosomal hexanucleotides of all known viral sequences is $13.2–37.6 \times 10^{-3}$ (Table 5). When the average probabilities were calculated in viral families, the minimum probability was 3.7×10^{-3} in Herpesviridae and the maximum probability was 44.8×10^{-3} in Poxviridae (Table 5). These median values of probabilities in viral genomes were greater than those of ribosomal RNAs (Table 4) and comparable with those of non-V00125 and random hexamers (Table 5). These data suggest that non-ribosomal hexanucleotides prime cDNA synthesis in most viruses.

Model experiment for differentiated amplification of viral RNA by cDNA RDA

The database analysis suggests that viral RNAs were efficiently primed by non-ribosomal hexanucleotides in comparison with ribosomal RNAs. We investigated the effect of non-ribosomal hexanucleotides on cDNA synthesis by using *in vitro* synthesized plasmid RNA (artificial RNA) and total cellular RNA, including ribosomal RNAs. An autoradiogram of ^{32}P-labelled double-stranded cDNAs that were synthesized using non-ribosomal hexanucleotides or a random primer and subsequently separated by agarose gel electrophoresis is shown in Figure 2. When test and total cellular RNAs were reverse transcribed individually, the efficiencies of cDNA synthesis from artificial RNA using random and non-ribosomal hexanucleotides were almost similar; however, the efficiency of cDNA synthesis of cellular RNA was markedly lower in a non-ribosomal hexanucleotide-primed cDNA sample than in a random primer-primed cDNA sample (Figure 2A). In the mixed samples of test and total cellular RNAs, ribosomal RNAs were inefficiently reverse transcribed with non-ribosomal hexanucleotides. The total incorporated counts in non-ribosomal hexanucleotides-primed cDNAs decreased with a decrease in the proportion of the test RNA in the mixed RNA samples (Figure 2A). It is considered that the efficiency of reverse transcription depends on the proportions of the test RNA in the mixed RNAs. When approximately the same counts of cDNAs were loaded on the gel, synthesis of ribosomal RNA-derived cDNA (ribosomal cDNA) was obvious in random primer-primed cDNAs (Figure 2B).